Available online at www.sciencedirect.com
SCIENCE DIRECT®
Journal of Organometallic Chemistry 690 (2005) 6178–6204
Journal of Organometallic Chemistry
www.elsevier.com/locate/jorganchem

Chemical bonding in transition metal carbene complexes ☆

Gernot Frenking [a,*], Miquel Solà [b,*], Sergei F. Vyboishchikov [b,*]

[a] Fachbereich Chemie, Philipps-Universität Marburg, Hans-Meerwein-Strasse, D-35032 Marburg, Germany
[b] Institut de Química Computacional and Department de Química, Universitat de Girona, E-17071 Girona, Catalonia, Spain

Received 22 June 2005; received in revised form 29 August 2005; accepted 29 August 2005
Available online 8 November 2005

Abstract

In this work, we summarize recent theoretical studies of our groups in which modern quantum chemical methods are used to gain insight into the nature of metal–ligand interactions in Fischer- and Schrock-type carbene complexes. It is shown that with the help of charge- and energy-partitioning techniques it is possible to build a bridge between heuristic bonding models and the physical mechanism which leads to a chemical bond. Questions about the bonding situation which in the past were often controversially discussed because of vaguely defined concepts may be addressed in terms of well defined quantum chemical expressions. The results of the partitioning analyses show that Fischer and Schrock carbenes exhibit different bonding situations, which are clearly revealed by the calculated data. The contributions of the electrostatic and the orbital interaction are estimated and the strength of the σ donor and π acceptor bonding in Fischer complexes are discussed. We also discuss the bonding situation in complexes with N,N-heterocyclic carbene ligands.

Keywords: Bonding analysis; Energy decomposition analysis (EDA); Charge decomposition analysis (CDA); Dewar–Chatt–Duncanson model; Bond strength

1. Introduction

Forty years have passed since the epochal synthesis of the first transition metal (TM) carbene complex $(CO)_5Cr$–C(OMe)(Me) by Fischer and Maasböl in 1964 [1]. The new class of compounds soon proved very useful and versatile for organic and organometallic synthesis [2]. Ten years later, Schrock [3] introduced another chemically and industrially important class of compounds with a metal–carbon double bond when he reported the synthesis of $(Me_3CCH_2)_3Ta$–C(H)(CMe_3). It was soon recognized that the Schrock carbenes behave, chemically, very different to the Fischer carbenes [4]. The carbene ligands of the latter species are usually electrophilic, while the former compounds have a nucleophilic center. Stable Fischer carbenes usually have a stabilizing π-donor substituent (typically OR or NR_2) at the carbene ligand while Schrock carbenes do not. Also, the metal in a Fischer carbene is typically in a low oxidation state while Schrock carbenes have metals in a higher oxidation state. The metal–carbene bonding in the former class of compounds is usually discussed in terms of the familiar Dewar–Chatt–Duncanson (DCD) donor–acceptor model [5] which considers the dominant bonding interactions to arise from ligand → metal σ donation and metal → ligand π back-donation. A schematic representation of the DCD model for Fischer-type carbene complexes is shown in Fig. 1(a).

In contrast to Fischer carbenes, bonding in Schrock-type carbene complexes is better described as a covalent bond between a triplet carbene and a triplet metal fragment as shown in Fig. 1(b) [6]. Since the latter model does not employ donor–acceptor interactions between the metal and the fragment, Schrock carbenes are better named alkylidenes. A particular subclass of Fischer complexes have carbene ligands which need little π back-donation from the

☆ Theoretical Studies of Organometallic Compounds. 53. Part 52: D. Nemcsok, K. Wichmann, G. Frenking, Organometallics 23 (2004) 3640.

* Corresponding authors. Tel.: +49 6421 2825563; fax: +49 64212825561.
E-mail addresses: frenking@chemie.uni-marburg.de (G. Frenking), miquel.sola@udg.es (M. Solà), vybo@stark.udg.es (S.F. Vyboishchikov).

0022-328X/$ - see front matter © 2005 Elsevier B.V. All rights reserved.
doi:10.1016/j.jorganchem.2005.08.054

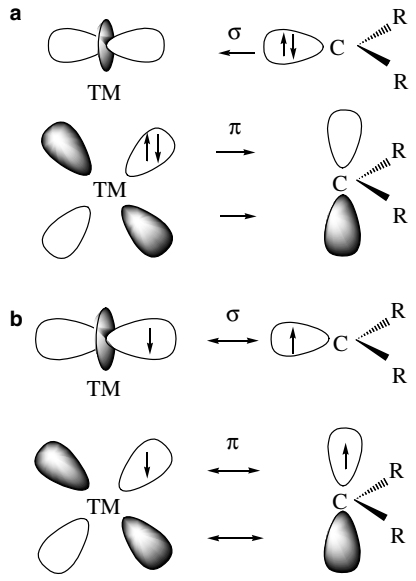

Fig. 1. Schematic representation of the dominant orbital interactions in: (a) Fischer-type carbene complexes and (b) Schrock-type carbene complexes.

metal to be stable enough to be isolated and where the carbene ligands can even be synthesized as free species. These are complexes of N,N-heterocyclic carbenes (imidazol-2-ylidenes) and related compounds which are known since the pioneering work of Öfele [7] and Wanzlick [8,9].

Besides the spectacular advancements in the experimental research of transition metal carbene complexes, much progress has been made in recent years in understanding the electronic structure and bonding situation of the compounds [10]. Modern quantum chemical methods have been employed to gain insight into the metal–carbene bonding of Fischer and Schrock carbenes. The results of charge and energy partitioning analyses which have been used in our groups make it possible to address questions about the nature of the bonding such as electrostatic versus covalent interactions and the strength of σ donation and π back-donation quantitatively using well defined quantum chemical methods. The methods which will be introduced and whose results will be discussed below serve as a bridge between the physical mechanism of bond formation and the heuristic bonding models which historically became developed through the neuronal net of correlating experimental observations with ad hoc assumptions. The bonding models for Fischer and Schrock carbenes shown in Fig. 1 have been examined and the results were expressed in terms of well-defined quantum chemical terms which provide a quantitative estimate of the orbital interactions.

The present situation should not be considered as something which could have been expected because of the progress in quantum chemistry. In an earlier work about the electronic structure of transition metal carbene complexes, Peter Hofmann expressed serious doubts that accurate ab initio calculations could ever become subject to an interpretation of the electronic structure aiming at qualitative understanding of the bonding situation: "Many variants of ab initio techniques using different basis sets and varying approaches to go beyond the HF limit, utilizing all-electron or pseudopotential formalisms of both relativistic and non-relativistic type, are now being evolved by theoretical groups specializing in the calculation of the electronic structure of organometallics. Theory will undoubtedly devise ever more efficient and accurate methods. A complementary disadvantage of this development, however, seems to be that work of this type is becoming increasingly difficult to interpret and understand in terms of simple qualitative concepts of bonding [11]." The present work shows the progress which has been made in the meantime which strikingly refutes the latter statement.

In this paper, we summarize the results of our quantum chemical studies of transition metal carbene complexes which we published in recent years [12–16]. The main working horses of the bonding analyses are the charge decomposition analysis (CDA) developed by Dapprich and Frenking [17] and the energy decomposition analysis (EDA) of the program ADF [18] which is based on the methods suggested by Ziegler and Rauk [19] and Morokuma [20]. Other important methods for the electronic structure analysis which were employed are the topological analysis of the electron density distribution which is also-called atoms in molecules (AIM) theory developed by Bader [21] and the natural bond orbital (NBO) method of Weinhold and co-workers [22]. The investigated molecules are examples for Fischer-, Schrock- and Öfele/Wanzlick-type carbene complexes. We also discuss the bonding situation in heavy-atom analogues of carbene complexes $L_nTM–ER_2$ (E = Si, Ge, Sn, Pb).

It is fair to emphasize that other groups also contributed in the past with important theoretical investigations to the present knowledge about the chemical bonding in carbene complexes. In particular, we want to point out four ground breaking studies by Cundari and Gordon [23] who analyzed the metal–ligand bonding situation in carbene complexes and higher group-14 homologues with a multiconfigurational wavefunction. Another important contribution came from the Ziegler group [24] who reported about EDA calculations of the bonding in transition metal complexes $(CO)_5TM–ER_2$ (TM = Cr, Mo, W, Mn^+; E = C, Pb; R = H, F, Cl, Me, OMe). Several other groups published theoretical work which gave insight into the nature of metal–carbene bonding [25]. Further theoretical studies of carbene complexes have been published which focussed, however, on energies, geometries and other molecular properties but not on the bonding situation.

2. Methods

The results which are reported here have been obtained from quantum chemical ab initio and DFT calculations at various theoretical levels. The ab initio calculations were carried out mostly using second-order Møller–Plesset perturbation theory (MP2) [26] or using coupled-cluster theory at the CCSD(T) level [27]. For the DFT calculations

the BP86 [28] and B3LYP [29] functionals were employed. The quality of the basis sets varies between valence DZP and TZ2P. Relativistic effects have been considered for the heavier atoms by using the ZORA approximation [30] or by using relativistic effective core potentials [31]. Further details of the calculations can be taken from the original publications.

Various charge and energy partitioning methods were employed for gaining insight into the bonding situation of the carbene complexes. We think that all methods have their strength and weakness and that the choice should be made with a good knowledge of the underlying approach and the technical details of the procedure in order to avoid an over- or misinterpretation of the results.

The NBO method [22] has been designed to give a quantitative interpretation of the electronic structure of a molecule in terms of Lewis structures. Since Lewis structures are popular bonding models in chemistry the NBO method is frequently chosen for the interpretation of the bonding situation. One advantage of the NBO analysis is that the results are quite robust against changing the basis set. However, it is important to recognize that the algorithm for the transformation of the wavefunction into Lewis structures [32] contains an weighting factor which automatically disfavours atomic basis functions which are empty in the atomic ground state in the description of the chemical bond. Thus, the NBO method excludes a priori the outermost d orbitals of the heavier main group elements and the outermost p orbitals of the TMs from the valence space. It has been shown by Maseras and Morokuma [33] that the outermost p orbitals of the transition metals become significantly occupied if they are part of the valence functions during the orthogonalization procedure. Thus, the results of the NBO method cannot be used to investigate the question whether the d functions of main group elements and the p functions of the TMs are true valence orbitals or polarization functions, because the answer is already enforced by the preselection of the orbitals belonging to the valence space in the occupancy-weighted orthogonalization.

The CDA method of Dapprich and Frenking [17] can be seen as a quantitative expression of the DCD model [5] of synergistic metal–ligand bonding, which considers the ligand $\rightarrow$ metal σ donation and ligand $\leftarrow$ metal π back-donation as the dominant factors for the metal–ligand bond. In the CDA, the wavefunction of a complex L_nTM–X is expressed as a linear combination of the fragment molecular orbitals of the ligand X and the remaining metal fragment L_nTM both in closed-shell configurations. The orbital contributions of the fragments to wavefunction of the complex are divided into four parts: (i) mixing of the occupied MOs of X and the unoccupied MOs of L_nTM (donation $X \rightarrow TML_n$); (ii) mixing of the unoccupied MOs of X and the occupied of L_nTM (back-donation $X \leftarrow TML_n$); (iii) mixing of the occupied MOs of X and the occupied MOs of L_nTM (repulsive polarization $X \leftrightarrow TML_n$); (iv) mixing of the unoccupied MOs of X and the unoccupied MOs of L_nTM (rest term Δ). The latter term should not contribute to the electronic structure of the complex. It has been found that the rest term is a sensitive probe if the compound can be classified as a donor–acceptor complex [34]. A significant deviation from $\Delta = 0$ indicates that the bond L_nTM–X has the character of a normal covalent bond between two open-shell fragments, rather than a donor–acceptor bond between a Lewis acid and Lewis base. The CDA may be used in conjunction with HF and natural orbitals from correlated calculations and with Kohn–Sham orbitals given by DFT calculations. Early test calculations showed that the CDA results do not change significantly when the basis set becomes larger [17]. However, more recent work has shown that the CDA may deteriorate with larger basis sets [35].

A theoretical tool for analyzing the electronic structure of a molecule which is not based on orbitals but rather on the electron density distribution is the AIM method of Bader [21]. The central idea of AIM is that the topology of the electron density distribution $\rho(\mathbf{r})$ contains information about the bonding situation which can be elucidated when $\rho(\mathbf{r})$ becomes the subject of a mathematical analysis. It has been shown that the topological analysis of $\rho(\mathbf{r})$, its first derivative (gradient field) $\nabla\rho(\mathbf{r})$ and second derivative (Laplacian) $\nabla^2\rho(\mathbf{r})$ reveals helpful information about the electronic structure of a molecule. Another very attractive feature of the AIM method is that the results of the topological analysis give directly the atomic subspaces (basins) of a molecule and the bonding connectivity between the atoms. Atomic basins are defined as the regions in Cartesian space that are bordered by zero-flux surfaces in the gradient of the electron density. The position of the atomic nucleus is defined in the AIM model as a critical point in the three-dimensional space where the first derivatives $\nabla\rho(\mathbf{r})$ are zero and the eigenvalues of the second derivative matrix of $\rho(\mathbf{r})$ are all negative.

The correspondence between orbital concepts and electron distributions was analyzed [36] and attempts have been made to establish links between the AIM method and classical bonding models such as bond order. Cioslowski and Mixon [37] proposed covalent bond orders which are based on partitioning of the number of electrons within the topological theory of AIM.

Another important development of AIM based models for the interpretation of the bonding situation are the localization indices (LIs) and delocalization indices (DIs) which, at the HF and DFT level, are calculated as [38]

$$\lambda(\mathrm{A}) = 2\sum_{i,j}(S_{ij}(\mathrm{A}))^2, \tag{1}$$

$$\delta(\mathrm{A},\mathrm{B}) = 4\sum_{i,j} S_{ij}(\mathrm{A})S_{ij}(\mathrm{B}), \tag{2}$$

where $S_{ij}(\mathrm{A})$ is the overlap of the molecular orbitals (MO) i and j in the basin of atom A, and the summations run over all the occupied MO's. The localization index (LI), $(\lambda)(\mathrm{A})$, is the number of electrons which are completely localized in an atom A, while the delocalization index (DI), $(\delta)(\mathrm{A},\mathrm{B})$ is the number of electrons delocalized or shared between two atoms A and B.

Ponec and co-workers [39] reported an AIM generalization of these multicenter bond indices, the 3-center DI, which depends on the third-order electron density. At the HF (or approximate KS-DFT) level, this 3-center DI is expressed for A ≠ B ≠ C as

$$\delta(A,B,C) = 12\sum_{i,j,k} S_{ij}(A)S_{jk}(B)S_{ki}(C). \quad (3)$$

Ponec has used this DI to detect 3-center bonding in several molecules. Positive $\delta(A,B,C)$ values are characteristic of 3-center 2-electron (3c–2e) bonds, while negative values correspond to 3c–4e bonds. $\delta(A,B,C)$ is close to zero when no 3c-bonding between the three atoms is present [40].

The above introduced methods are different approaches for partitioning the electronic charge of a molecule into atomic or orbital domains. It is also possible to device partitioning schemes for the bonding interaction between atoms or fragments in a molecule. Since energy is the crucial factor for structure and reactivity, energy decomposition analyses are perhaps even more helpful for gaining information about the driving force leading to molecular geometry and reactivity. One such method is the EDA of ADF [18] which was originally developed by Morokuma [20] and later modified by Ziegler and Rauk [19]. The focus of the bonding analysis is the instantaneous interaction energy, ΔE_{int}, of the bond, which is the energy difference between the molecule and the fragments in the frozen geometry of the compound. The interaction energy can be divided into three main components

$$\Delta E_{int} = \Delta E_{elstat} + \Delta E_{Pauli} + \Delta E_{orb}, \quad (4)$$

where ΔE_{elstat} gives the electrostatic interaction energy between the fragments, which are calculated using the frozen electron density distribution of the fragments. This term is also-called quasi-classical electrostatic attraction according to Ruedenberg [41]. The second term in Eq. (4), ΔE_{Pauli}, refers to the repulsive interactions between the fragments, which are caused by the fact that two electrons with the same spin cannot occupy the same region in space. ΔE_{Pauli} is calculated by enforcing the Kohn–Sham determinant of the orbitals of the superimposed fragments to obey the Pauli principle by antisymmetrization and renormalization. The stabilizing orbital interaction term, ΔE_{orb}, which includes the Heitler–London resonance phenomenon [42] but has additional contributions from polarization and relaxation is calculated in the final step of the energy partitioning analysis when the Kohn–Sham orbitals relax to their optimal form. This term can be further partitioned into contributions by the orbitals belonging to different irreducible representations of the point group of the interacting system. The interaction energy, ΔE_{int}, can be used to calculate the bond dissociation energy, D_e, by adding ΔE_{prep}, which is the energy necessary to promote the fragments from their equilibrium geometry to the geometry in the compounds (Eq. (5)) [43]. Further details about the EDA can be found in the literature [18]

$$-D_e = \Delta E_{prep} + \Delta E_{int}. \quad (5)$$

The EDA has been used in the past mainly for analyzing the interactions between closed-shell species. Recent work has shown that the method is also very useful for analyzing electron-sharing (covalent) bonds between open-shell fragments [44,45,56,57].

The calculations which are reported here have been performed using the quantum chemical program packages ADF [18], Turbomole [46], ACES-II [47], and various versions of GAUSSIAN [48]. For the CDA calculations the program CDA-2.1 has been employed [49]. The AIM calculations were performed with the program AIMPAC [50].

3. Charge- and energy decomposition analysis of Fischer complexes $(CO)_5Cr–C(X)R$

It is appropriate to begin the discussion of the bonding situation in carbene complexes with the first compound which was isolated by Fischer in 1964, i.e., $(CO)_5Cr–C(Me)OMe$. The nature of the metal–carbene bonding in the complex and in the substituted analogues $(CO)_5Cr–C(X)R$ where X = H, OH, OMe, NH_2, NHMe and R = H, Me, CH=CH_2, Ph, C≡CH was analyzed with the CDA and EDA methods by Cases et al. [12] (see Fig. 2). The theoretical study of the 25 carbene complexes was carried out using density functional theory at the BP86 level using double-zeta basis sets (in some cases triple-zeta basis sets) which are augmented by one set of polarization functions. Further details of the method and the full geometries of the optimized structures can be found in the original publication [12].

The qualitative bonding model for Fischer complexes is shown in Fig. 1(a). The DCD model considers for the bonding two synergistic interactions, i.e., carbene → metal σ donation and metal → carbene π back-donation. The pivotal question concerns the relative strength of the two bonding components. The answer can be given in terms of charge donation, i.e., how much electronic charge is donated in each direction. Another possibility is to focus on the associated energy which contributes to the overall metal–carbene binding. The first question has been addressed with the CDA method. Table 1 shows the calculated σ donation and π back-donation and their ratio for the 25 complexes **A**–**Y**.

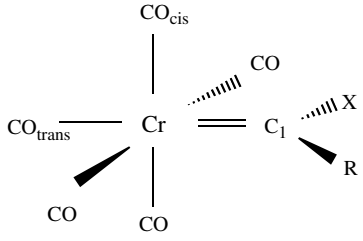

Fig. 2. Schematic representation of a Fischer-type chromium–carbene complex.

Table 1
Calculated charge donation d, back-donation b, donation/back-donation ratio d/b, and repulsive polarization r of the complexes Fischer carbene complexes $(CO)_5Cr–C(X)R$ **A**–**Y** obtained from the CDA analysis[a]

	X	R	d	b	d/b	r
A	OCH_3	H	0.528	0.244	2.165	−0.319
B	OH	H	0.499	0.255	1.957	−0.342
C	$NHCH_3$	H	0.511	0.218	2.342	−0.299
D	NH_2	H	0.501	0.214	2.342	−0.317
E	H	H	0.501	0.284	1.764	−0.358
F	OCH_3	CH_3	0.536	0.218	2.457	−0.327
G	OH	CH_3	0.525	0.227	2.315	−0.334
H	$NHCH_3$	CH_3	0.524	0.190	2.755	−0.299
I	NH_2	CH_3	0.527	0.207	2.545	−0.295
J	H	CH_3	0.518	0.267	1.942	−0.325
K	OCH_3	$CH{=}CH_2$	0.522	0.206	2.532	−0.334
L	OH	$CH{=}CH_2$	0.507	0.215	2.358	−0.328
M	$NHCH_3$	$CH{=}CH_2$	0.502	0.191	2.632	−0.309
N	NH_2	$CH{=}CH_2$	0.499	0.198	2.519	−0.313
O	H	$CH{=}CH_2$	0.508	0.240	2.119	−0.348
P	OCH_3	Ph	0.513	0.243	2.110	−0.344
Q	OH	Ph	0.503	0.249	2.020	−0.335
R	$NHCH_3$	Ph	0.486	0.214	2.272	−0.315
S	NH_2	Ph	0.480	0.229	2.096	−0.324
T	H	Ph	0.492	0.263	1.869	−0.365
U	OCH_3	C≡CH	0.391	0.205	1.908	−0.323
V	OH	C≡CH	0.469	0.222	2.114	−0.339
W	$NHCH_3$	C≡CH	0.404	0.205	1.972	−0.306
X	NH_2	C≡CH	0.391	0.193	2.024	−0.307
Y	H	C≡CH	0.496	0.258	1.923	−0.268

Units in electrons.
[a] Values are taken from [12].

The calculated values for the σ donation are relatively constant between 0.528 and 0.480 electrons, except for systems with R = C≡CH which have lower values for the donation which can be explained with the significantly σ-withdrawing character of the substituent [51]. Note that complexes with R = Me exhibit the largest values for σ-donation which can be expected from the σ electron donating character of the methyl group. Unlike donation, values of charge back-donation are more spread over a broad range of values varying from 0.284 to 0.190. For a given R, back-donation increases in the order H > OH > OMe > NH_2 > NHMe, that is, it becomes more intense with the decrease of the π donor character of the X group. The reduction of back-donation for systems with the phenyl group as substituent which is a π electron donor [52] is not observed because the non-coplanarity of the phenyl group within the carbene ligand impedes π electron donation from the phenyl group. The low back-donation values of Fischer carbene complexes with R = C≡CH are somewhat unexpected given the π-acceptor nature of this group and are attributed to the reduced σ donation that in these systems partially blocks the synergetic mechanism that favors back-donation. A previous CDA study of complexes $TM(CO)_5L$ (TM = Cr, Mo, W; L = CO, SiO, CS, N_2, NO^+, CN^-, NC^-, HCCH, CCH_2, CH_2, CF_2, H_2) showed that the TM → L back-donation correlates indeed quite well with the change of the TM–CO_{trans} bond length while the L → TM donation does not [53]. We plotted the calculated metal → carbene π back-donation in the 25 complexes $(CO)_5Cr–C(X)R$ as a function of the Cr–$C_{carbene}$, Cr–CO_{trans}, and C–O_{trans} bond distances. The results are shown in Fig. 3.

Fig. 3 clearly shows that the $(CO)_5Cr–C(X)R$ complexes with X substituents having higher π-donor character show smaller back-donation values, larger Cr–$C_{carbene}$ and C–O_{trans} bond lengths, and shorter Cr–CO_{trans} bond distances. Attempts to correlate carbene → metal σ donation values led to poor results. The greater influence of back-donation on the structural properties of the complexes may be attributed to the fact that donation values are almost uniform for all complexes analyzed, whereas charge back-donation numbers are more dispersed over a wide range of values. Actually, most complexes failing to agree with the correlations presented in Fig. 3 are those having R = C≡CH that, as above-mentioned, have charge donation values lower than the common transfer of ca. 0.5 electrons.

Besides the charge decomposition analysis, the nature of the metal–carbene bonding in the 25 complexes was also investigated by Cases et al. [12] with an energy decomposition analysis. Table 2 gives the results of the EDA calculations. The pivotal energy term for the analysis is the instantaneous interaction energy ΔE_{int} between the carbene ligand and the metal fragment. The values for the preparation energy ΔE_{prep} do not change very much for different substituents which means that the ΔE_{int} values directly correlate with the trend of the bond strength.

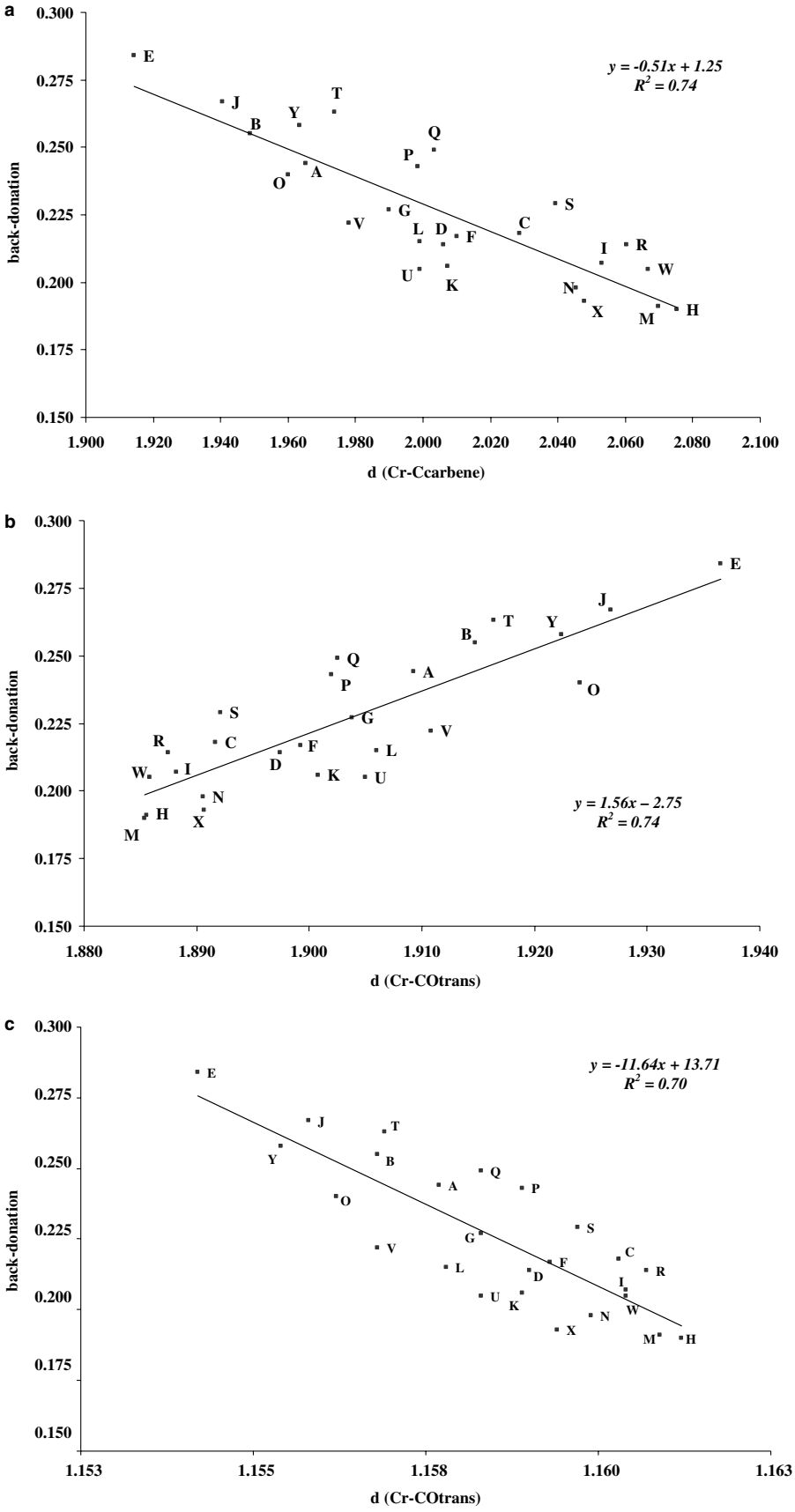

Fig. 3. Linear correlation of theoretical data of $(CO)_5Cr–C(X)R$ bonding: (a) Back-donation values from the CDA vs. the Cr–C(X)R bond distance (Å). (b) Back-donation values from the CDA vs. the $Cr–CO_{trans}$ bond distance(Å). (c) Back-donation values from the CDA vs. the $C–O_{trans}$ bond distance (Å). Reproduced with permission from [12]. See Table 2 for identifying the entries **A**–**Y**.

Table 2
Results of the energy decomposition analysis for the $(CO)_5Cr–C(X)R$ complexes **A**–**Y**[c]

	ΔE_{int}	ΔE_{Pauli}	ΔE_{elstat}[a]	ΔE_{orb}[a]	ΔE_{σ}[b]	ΔE_{π}[b]	ΔE_{prep}	$\Delta E(=-D_e)$
A	−79.8	168.3	−153.3 (61.8)	−94.8 (38.2)	−66.7 (70.0)	−28.6 (30.0)	3.4	−76.4
B	−81.0	175.7	−158.0 (61.5)	−98.7 (38.5)	−67.8 (68.2)	−31.7 (31.8)	3.2	−77.8
C	−76.5	154.0	−148.8 (64.6)	−81.7 (35.4)	−66.5 (78.6)	−18.1 (21.4)	2.7	−73.9
D	−76.1	161.7	−152.9 (64.3)	−84.9 (35.7)	−67.2 (76.9)	−20.2 (23.1)	2.9	−68.7
E	−102.6	199.6	−175.4 (58.0)	−126.8 (42.0)	−72.3 (57.2)	−54.1 (42.8)	4.7	−97.9
F	−75.9	161.3	−149.2 (62.9)	−88.0 (37.1)	−64.1 (73.1)	−16.7 (26.9)	2.5	−73.4
G	−74.9	164.8	−148.7 (62.0)	−91.0 (38.0)	−65.8 (71.6)	−26.0 (28.4)	3.5	−71.4
H	−75.2	147.8	−144.5 (64.8)	−78.5 (35.2)	−63.6 (80.6)	−15.3 (19.4)	2.8	−72.4
I	−72.6	151.4	−144.0 (64.3)	−80.0 (35.7)	−64.8 (79.5)	−16.7 (20.5)	2.7	−69.9
J	−96.0	195.8	−176.4 (60.5)	−115.4 (39.5)	−72.9 (62.5)	−43.8 (37.5)	5.5	−90.6
K	−73.6	159.2	−142.0 (61.0)	−90.8 (39.0)	−66.6 (73.2)	−24.4 (26.8)	3.0	−70.6
L	−75.6	161.7	−143.8 (60.6)	−93.5 (39.4)	−66.3 (70.1)	−28.4 (29.9)	3.6	−72.0
M	−70.0	143.2	−133.8 (62.8)	−79.4 (37.2)	−64.9 (79.8)	−16.5 (20.2)	2.6	−67.4
N	−70.0	148.7	−137.0 (62.6)	−81.7 (37.4)	−66.6 (77.9)	−18.9 (22.1)	2.5	−67.5
O	−98.0	189.4	−174.0 (60.5)	−113.4 (39.5)	−68.8 (63.4)	−37.7 (36.6)	3.3	−94.7
P	−74.8	160.7	−142.7 (60.6)	−92.8 (39.4)	−66.1 (70.8)	−27.3 (29.2)	2.6	−72.2
Q	−73.5	157.7	−140.6 (60.8)	−90.6 (39.2)	−65.2 (69.5)	−28.7 (30.5)	3.3	−70.2
R	−70.9	143.9	−133.6 (62.2)	−81.2 (37.8)	−65.5 (78.7)	−17.7 (21.3)	2.5	−68.4
S	−70.9	149.6	−136.3 (61.8)	−84.2 (38.2)	−67.1 (81.5)	−15.3 (18.5)	4.0	−66.8
T	−91.8	186.2	−169.7 (61.0)	−108.3 (39.0)	−68.3 (58.9)	−47.7 (41.1)	4.3	−87.5
U	−73.1	153.4	−135.3 (59.7)	−91.2 (40.3)	−64.8 (70.7)	−26.9 (29.3)	3.0	−70.1
V	−74.7	160.2	−138.8 (59.1)	−96.1 (40.9)	−66.5 (68.6)	−30.4 (31.4)	2.9	−71.8
W	−66.9	135.7	−125.5 (61.1)	−77.1 (38.1)	−64.3 (79.2)	−16.9 (20.8)	2.3	−64.7
X	−67.2	140.7	−128.1 (61.6)	−79.8 (38.4)	−62.6 (76.8)	−18.9 (23.2)	2.7	−64.5
Y	−85.3	165.2	−139.4 (55.6)	−111.1 (44.4)	−69.0 (61.8)	−42.7 (38.2)	3.9	−81.4

The values are given in kcal/mol.
[a] In parentheses, percentage of the total attractive interactions $\Delta E_{elstat} + \Delta E_{oi}$.
[b] In parentheses, percentage of the total orbital interactions ΔE_{oi}.
[c] Values are taken from [12].

The largest value for ΔE_{int} is calculated for the methylene complex $(CO)_5Cr–CH_2$ (**E**) (Table 2) which has not been isolated so far. It is known that Fischer-type carbene complexes can only become isolated if the carbene ligand bears at least one π-donor substituent [2]. The calculated data clearly show that the chemical stability of the complexes is *not* related to the strength of the metal–carbene bond.

There are three energy terms which contribute to the overall interaction energy ΔE_{int}, i.e., the repulsive Pauli term ΔE_{Pauli}, the electrostatic attraction ΔE_{elstat}, and the orbital interaction ΔE_{orb}. It has been suggested that the relative values of the latter two attractive terms may be used to characterize the nature of the chemical bond [54] The values in Table 2 show that the metal–carbene bond has a large electrostatic character. The ΔE_{elstat} term contributes between 55.6% (**Y**) and 64.6% (**C**) to the attractive interactions. It is tempting to correlate the electrostatic term with ionic interactions, which would indicate that the carbene complexes **A**–**Y** would have a pronounced ionic character. The conclusion is not justified, however, because strong electrostatic attraction is also found in nonpolar bonds [55–57]. At shorter interatomic distances where the orbital overlap becomes larger, the electron–electron repulsion becomes less than the values which are given by a point-charge approximation which is still valid for the nuclear–nuclear repulsion. This yields an overall significantly attractive electrostatic interaction even for nonpolar bonds between identical atoms or fragments. For example, the electrostatic attraction between the nitrogen atoms in N_2 has been calculated as >320 kcal/mol [55–57]. A more detailed discussion of this can be found in the literature [18b,57,58].

The ΔE_{orb} term thus contributes according to the EDA results only between 35.4% and 44.4% to the metal–carbene attraction in **A**–**Y**. It is worth noting that in many cases but not always stronger orbital interactions and shorter bonds translate into higher bond dissociation energies, because the electrostatic attraction and the Pauli repulsion play also a role when differences in ΔE_{orb} are small [59]. For example, complex **D** has a shorter $Cr–C_{carbene}$ bond distance (values of bond distances in [12]) and stronger orbital interactions (Table 2) than complex **C**, but the total interaction energy and the bond dissociation energy of complex **C** are larger than those of complex **D**.

Although the orbital term is only the minor contributor to the attractive interactions, we found that the ΔE_{orb} term correlates quite well with the change of the $Cr–C_{carbene}$ bond distance. Fig. 4 shows a plot of ΔE_{orb} term as a function of the metal–carbene distance which shows a good correlation. The previous CDA results suggests that an even better correlation might be found when only the π orbital part of ΔE_{orb} is considered. To analyze further the orbital interaction energy term, we have slightly modified the geometry of the optimized complexes (by changing only dihedral angles and freezing the rest of the geometrical parameters) in order to attain C_s symmetry. In this

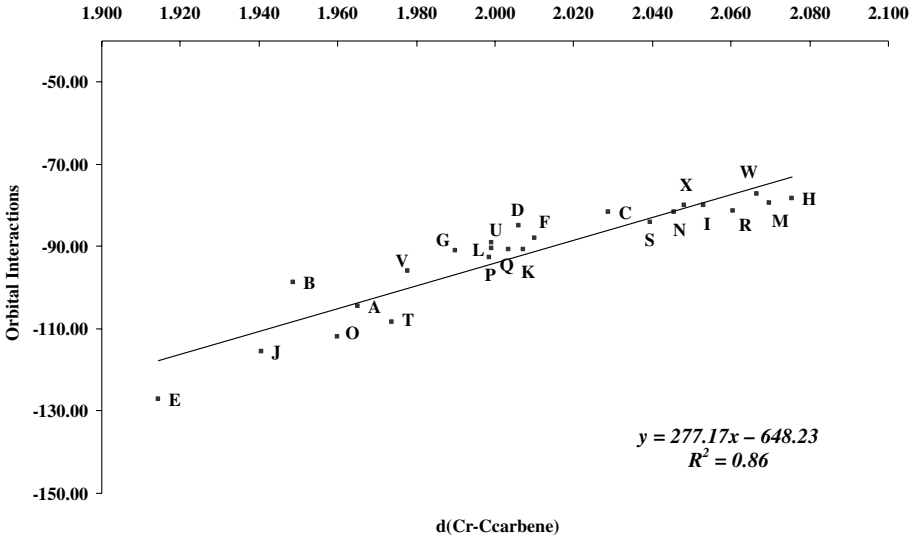

Fig. 4. Calculated values of the ΔE_{orb} term (kcal/mol) of the EDA vs. the metal–carbene bond distance (Å) of $(CO)_5Cr$–C(X)R. Reproduced with permission from [12].

geometrical arrangement, it is possible to separate the orbital interaction energy into the σ and π components. Because of the geometry changes the two σ and π terms added do not sum exactly the ΔE_{orb} gathered in Table 2. The energy differences between the C_1 equilibrium structures and the constrained C_s forms are very small (<1 kcal/mol) and thus, they can be neglected for the discussion.

From the results in Table 2, we can see that, first, the component connected with donation (ΔE_σ) is more than twice as large as the term associated with back-donation (ΔE_π); and second, ΔE_π values are more scattered over a broad range of values, whereas ΔE_σ values are more uniform. As expected, the geometrical parameters correlate even better with ΔE_π values (Fig. 5) than with the full ΔE_{orb} term (Fig. 4). This is in agreement with the conclusions obtained from the CDA calculations. In general, correlations of ΔE_π energies versus Cr–$C_{carbene}$, Cr–CO_{trans}, or C–O_{trans} bond lengths (the latter are not shown here) are quantitatively better than those generated using the charge back-donation values obtained from the CDA calculations. Qualitatively, however, correlations of Fig. 3(b) and Fig. 5 are quite similar. We find the same grouping of complexes in the two representations, and, in particular, it is found that for a fixed R substituent, the π component of the charge or the energy decomposition analysis decreases (in absolute value) when we have a stronger π-donor substituent, i.e., in the order H > OH > OMe > NH_2 > NHMe.

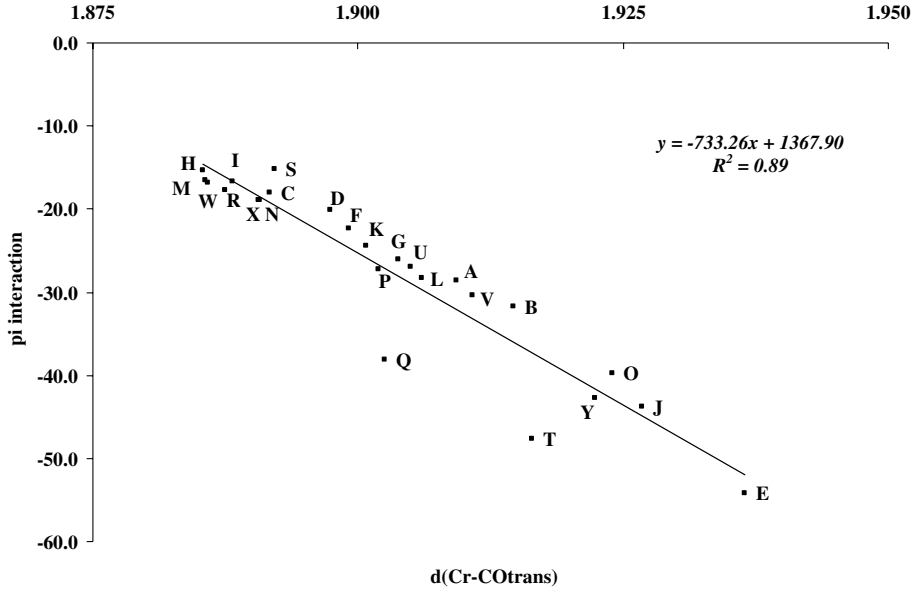

Fig. 5. Calculated π contribution to the orbital interaction term ΔE_{orb} (kcal/mol) vs. the Cr–CO_{trans} bond distance (Å) of $(CO)_5Cr$–C(X)R. Reproduced with permission from [12].

An important property of Fischer carbene complexes is their electrophilic character. Since the donation is larger than back-donation, these carbene complexes formally have a $(CO)_5Cr^{\delta-} \leftarrow C^{\delta+}(X)R$ charge separation, which indicates an electron-deficient carbene carbon atom and suggest an electrophilic reactivity of the carbene site [60]. In order to evaluate the electrophilicity of these complexes, we have calculated the electrophilicity index, ω, for each complex measured according to Parr et al. [61] using the following expression:

$$\omega \equiv \mu^2/2\eta, \tag{6}$$

where μ is the chemical potential (the negative of the electronegativity) and η is the hardness [62]. Chemical potential and hardness can be calculated from the HOMO and LUMO orbital energies using the following approximate expressions [62]:

$$\mu = (\varepsilon_{LUMO} + \varepsilon_{HOMO})/2, \tag{7}$$

$$\eta = \varepsilon_{LUMO} - \varepsilon_{HOMO}. \tag{8}$$

The values of the electrophilicity index in Table 3 show clearly that π-donor substituents reduce the electrophilicity of the complex, as a result of the acceptor orbital in carbene becoming occupied by π-donation. Thus, for a fixed R, the electrophilicity increases following the order: H > OH > OMe > NH_2 > NHMe, which is the same order of increasing back-donation. For a given X, the complex with R = Me has smaller electrophilic character because of the donating properties of the methyl group. On the contrary, Fischer carbenes with R = C≡CH have the largest electrophilicities, in line with the acceptor character of the C≡CH group.

To complement the CDA and EDA analyses, an electron pair study of the 25 Fischer carbene complexes of Table 1 has been carried out using the AIM theory [63]. The values of the atomic populations and localization and delocalization indices (LIs and DIs) at the B3LYP/6-311G** level of theory for the Cr=C–X moiety are given in Table 4. Molecular geometries were taken from [12].

According to the AIM analysis, the electron population in the Cr atom is practically constant for the series studied. Indeed, N(Cr) values for these compounds range from 22.8 to 22.9 e, which correspond to atomic charges between +1.1 and +1.2 e. For the C atom, the population takes values between 5.5 and 6.3 e, corresponding to charges

Table 3
Calculated electrophilicity indices ω of the Fischer carbene complexes $(CO)_5Cr$–C(X)R[a]

$(CO)_5Cr$–C(X)R	H	CH_3	CH=CH_2	Ph	C≡CH
OCH_3	4.595	4.050	5.221	4.606	7.109
OH	4.814	4.377	7.613	5.967	7.367
$NHCH_3$	3.250	3.059	3.763	3.538	5.422
NH_2	3.682	3.262	4.349	3.651	5.793
H	7.721	6.332	10.399	9.184	10.487

Units are in eV.
[a] Values are taken from [12].

Table 4
Selected atomic populations (N), localization (λ) and delocalization (δ) indices for the Fischer carbenes $(CO)_5Cr$–C(X)R complexes **A**–**Y** at the optimized geometries[a]

	N(Cr)	N(C)	N(X)	λ(Cr)	λ(C)	λ(X)	δ(Cr,C)	δ(C,X)	δ(C,R)	δ(Cr,X)	δ(Cr,R)	δ(Cr,C,X)
A	22.858	5.579	9.022	19.856	3.834	7.787	0.844	1.113	0.905	0.112	0.041	−0.028
B	22.817	5.605	9.053	19.828	3.854	8.001	0.880	1.100	0.922	0.118	0.044	−0.029
C	22.861	5.627	8.126	19.865	3.853	6.357	0.705	1.332	0.908	0.095	0.031	−0.018
D	22.851	5.629	8.122	19.862	3.857	6.503	0.732	1.323	0.919	0.102	0.035	−0.024
E	22.829	6.257	0.978	19.840	4.353	0.421	1.124	0.976	0.976	0.051	0.051	0.041
F	22.836	5.575	9.030	19.849	3.799	7.787	0.752	1.081	1.017	0.099	0.038	−0.010
G	22.871	5.592	9.047	19.883	3.808	7.974	0.788	1.078	1.019	0.100	0.038	−0.013
H	22.867	5.613	8.128	19.876	3.805	6.361	0.628	1.302	1.009	0.080	0.029	0.002
I	22.884	5.615	8.126	19.890	3.811	6.496	0.658	1.289	1.006	0.086	0.031	−0.005
J	22.824	6.210	0.991	19.831	4.259	0.429	1.009	0.956	1.095	0.046	0.050	0.034
K	22.817	5.569	9.021	19.833	3.771	7.774	0.736	1.089	1.058	0.097	0.043	−0.012
L	22.836	5.612	9.040	19.855	3.824	7.953	0.824	1.059	1.086	0.100	0.039	−0.014
M	22.872	5.621	8.128	19.880	3.790	6.355	0.623	1.303	1.045	0.081	0.035	−0.004
N	22.898	5.624	8.116	19.902	3.790	6.478	0.664	1.283	1.055	0.089	0.035	−0.011
O	22.831	6.227	1.007	19.835	4.248	0.434	0.910	0.944	1.282	0.040	0.047	0.030
P	22.859	5.570	9.021	19.864	3.777	7.775	0.758	1.090	1.006	0.100	0.038	−0.014
Q	22.840	5.611	9.049	19.855	3.818	7.962	0.752	1.069	1.061	0.093	0.034	−0.009
R	22.879	5.622	8.122	19.894	3.795	6.345	0.637	1.306	1.002	0.084	0.030	−0.007
S	22.874	5.614	8.121	19.884	3.792	6.484	0.668	1.300	0.992	0.088	0.031	−0.012
T	22.820	6.221	1.003	19.826	4.255	0.432	0.910	0.947	1.212	0.040	0.043	0.030
U	22.850	5.486	9.005	19.862	3.676	7.761	0.757	1.056	1.145	0.102	0.052	−0.018
V	22.856	5.506	9.015	19.867	3.688	7.941	0.795	1.057	1.153	0.106	0.052	−0.020
W	22.856	5.547	8.091	19.870	3.703	6.311	0.644	1.260	1.140	0.092	0.043	−0.016
X	22.853	5.542	8.095	19.873	3.706	6.461	0.664	1.253	1.143	0.093	0.043	−0.017
Y	22.829	6.128	0.946	19.848	4.164	0.393	0.934	0.931	1.318	0.040	0.065	0.028

Units are in electrons.
[a] Values are taken from [63].

between +0.5 and −0.3 e. Indeed, negative N(C) populations are found only for complexes with H as the substituent X, while complexes with π-donor substituents have C atoms with positive charges (from +0.4 to +0.5 e). In general, the positive charge in the Cr atom is partially compensated with slight negative charges in the carbonyl groups. LIs for the Cr and C atoms follow closely the trends found for the corresponding populations. For all the carbenes, λ(Cr) takes values between 19.8 and 19.9 e, which means that ca. 3 of the electrons associated to Cr are shared with other atoms. The λ(C) values are between 4.2 and 4.4, when X = H, and between 3.7 and 3.9, for the rest of X groups.

The delocalization indices DI provide additional information on the characteristics of the Cr–C bond. δ(Cr, C) decreases with increasing π-donor character of the X group and increasing back-donation. Thus, for a given R, δ(Cr, C) decreases in the order $H > OH > OCH_3 > NH_2 > NHCH_3$, with the only exception of complex **P** where δ^P(Cr, C) is slightly larger than δ^Q(Cr, C). For instance, complexes with X = H have δ(Cr, C) values between 0.91 and 1.12 e, while those with $X = NHCH_3$ have δ(Cr, C) values between 0.62 and 0.71 e. Although the Cr–C bond in these complexes is formally a double bond, δ(Cr, C) values within this range (0.6 to 1.1 e) are characteristic of single covalent bonds,

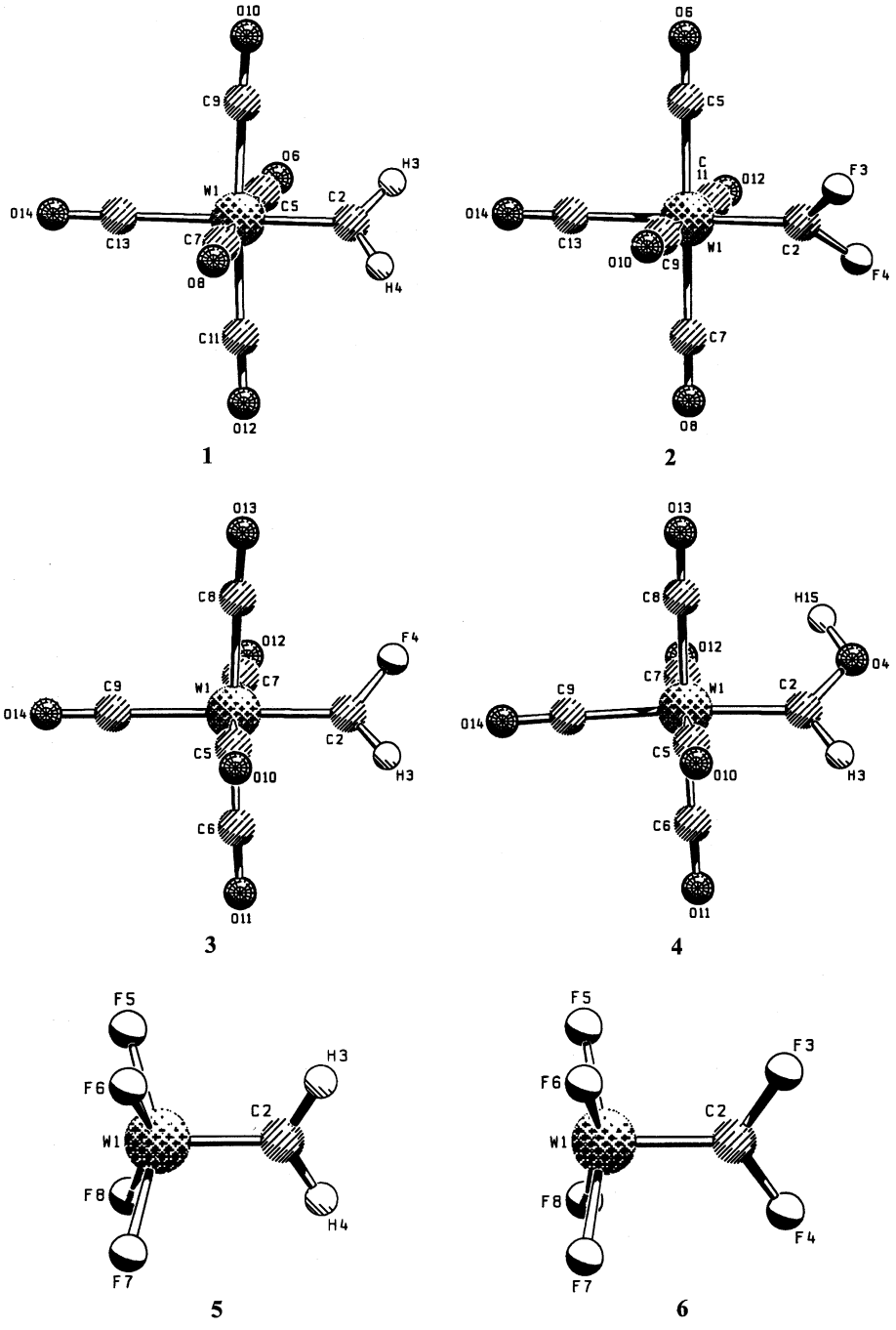

Fig 6. Optimized structures of the Fischer-type carbene complexes **1**–**4** and the Schrock-type carbenes **5**–**12**.

or bonds with little double bond character. However, bond polarization does also have a large influence on electron delocalization between bonded atoms. In fact, DIs between ionically bonded atoms are usually very small [38]. Both $\delta(C,X)$ and $\delta(C,R)$ take values between 0.9 and 1.3 e, which are typical of single bonds with partial double bond character. In general, $\delta(C,X)$ increases with the π-donor strength of the group X. Thus, as expected, an increase in the transfer of π electrons from X to C increases the double bond character in the C–X bond. For all the molecules, the σ component in $\delta(Cr,C)$ and $\delta(C,X)$ is more important than the π component [63]. However, the π component exhibits a larger variation along this series. Comparison of the values of EDA analysis with the DIs given in Table 4 reveal that back-donation measured as ΔE_π in Table 2 is directly proportional to $\delta(Cr,C)$, and inversely proportional to $\delta(C,X)$. In particular, the relationship between $\delta(Cr,C)$ and back-donation is especially strong ($r^2 = 0.903$).The correlation is even better between $\delta^\pi(Cr,C)$ and ΔE_π ($r^2 = 0.949$) [63].

It has been proposed that the π bond character of a metal–carbene can be better represented by a M–C–X

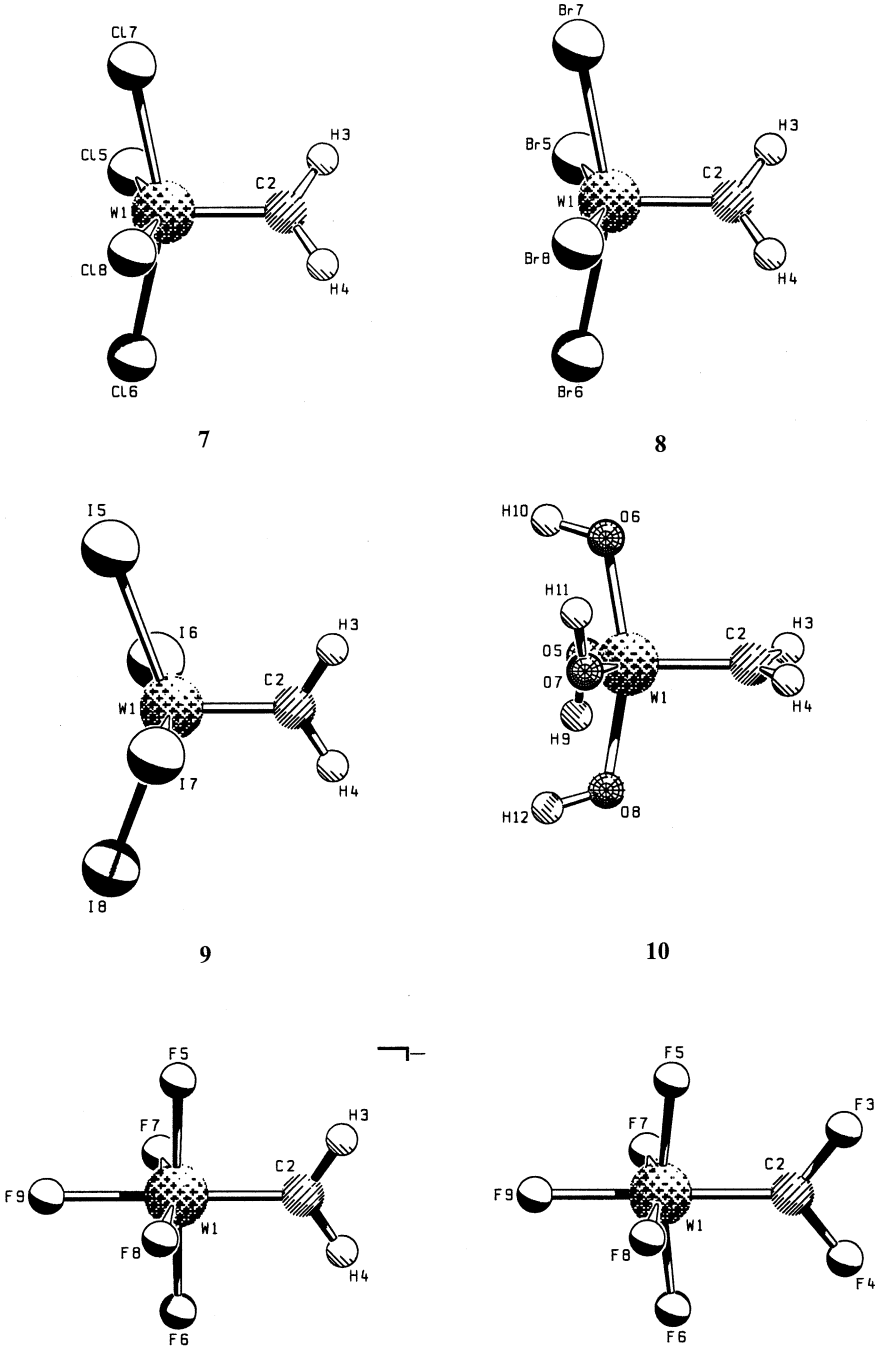

Fig. 6 (*continued*)

three-center four-electron (3c–4e) bond [64]. Additional information on the nature of the Cr–C–X interaction can be gained by examining the associated 3c-DI (Eq. (3)) (see Table 4). In most cases $\delta(Cr,C,X)$ is negative, except for the carbenes with X = H, and is minimal (ca. −0.03) for the carbenes **A** and **B**, which are also the ones with the largest $\delta(Cr,X)$ index. These results might indicate some degree of 3c–4e delocalization in these carbenes. In contrast, carbenes **E**, **J**, **O**, **T**, and **Y** exhibit $\delta(Cr,C,X)$ values between 0.03 and 0.04, and cannot be considered to have 3c–4e delocalization. The extent of the 3-center delocalization in all carbenes in this series may be considered low, in comparison to molecules which are usually attributed to have 3c–4e bonding interactions (e.g., N_3^-: −0.36; N_2O: −0.20) [39a,65]. Furthermore, one must be aware that non-bonded electron delocalization or 3-center delocalization have been found in many different molecules [38b]. For instance, this analysis also detects a low 3-center delocalization between the Cr atom and the carbonyl groups in this carbene series. Thus, it may be concluded that these systems present a weak 3c–4e bonding interaction character, which is incremented with the decrease of the π-donor character of the X group, except for X = H.

4. Electronic structure analysis of Fischer-type and Schrock-type carbene complexes

A comparative analysis of the nature of the chemical bonding in Fischer-type and Schrock-type carbene complexes was the subject of a theoretical study by Vyboishchikov and Frenking (VF) [14]. The authors analyzed the electronic structure of four Fischer-type and eight

Table 5
Results of the topological analysis of the electron density distribution of the carbene complexes **1**–**12** (Fig. 4) at the MP2/II level[a]

	Bond	$\rho(r_c)$	$\nabla^2\rho(\mathbf{r}_c)$	$H(\mathbf{r}_c)$	ε_c	Bond order[b]	d_c[c]
1	W–C2	0.885	6.580	−0.382	0.122	1.18	0.481
	W–C5	0.700	9.453	−0.198	0.115	0.82	–
	W–C13	0.632	8.327	−0.164	0.512	0.76	–
2	W–C2	0.775	9.446	−0.256	0.154	0.93	0.489
	W–C5	0.700	9.809	−0.197	0.032	0.84	–
	W–C13	0.667	9.376	−0.178	0.291	0.81	–
3	W–C2	0.873	8.216	−0.355	0.127	1.10	0.515
	W–C5	0.702	9.757	−0.199	0.072	0.84	–
	W–C9	0.629	8.652	−0.159	0.383	0.75	–
4	W–C2	0.770	7.464	−0.272	0.123	0.93	0.490
	W–C5	0.701	9.769	−0.198	0.044	0.86	–
	W–C9	0.670	9.139	−0.184	0.224	0.82	–
5	W–C	1.374	0.920	−0.940	0.549	1.71	0.444
	W–F	1.018	20.417	−0.242	0.0931	0.72	–
6	W–C	1.267	3.969	−0.793	1.147	1.54	0.464
	W–F	1.024	20.669	−0.247	0.140	0.74	–
7	W–C	1.404	0.576	−0.973	0.500	1.82	0.440
	W–Cl	0.655	5.639	−0.172	0.080	0.90	–
8	W–C	1.392	1.099	−0.956	0.486	1.85	0.441
	W–Br	0.553	3.195	−0.159	0.063	0.97	–
9	W–C	1.412	1.371	−0.978	0.450	1.87	0.443
	W-15	0.484	1.178	−0.155	0.053	1.11	–
	W-16	0.427	1.453	−0.126	0.018	1.03	–
10	W–C	1.289	1.991	−0.831	0.530	1.67	0.451
	W–O5	0.958	14.665	−0.273	0.195	0.82	–
	W–O6	0.911	14.997	−0.237	0.105	0.79	–
	W–O7	0.958	14.665	−0.274	0.195	0.78	–
11	W–C	1.184	3.589	−0.702	0.666	1.48	0.464
	W–F5	0.992	20.212	−0.212	0.036	0.66	–
	W–F7	0.897	17.427	−0.168	0.104	0.49	–
12	W–C	1.043	7.044	−0.530	0.393	1.57	0.476
	W–F5	0.934	18.769	−0.181	0.094	0.60	–
	W–F9	0.830	16.998	−0.134	0.240	0.58	–

[a] Electron density at the bond critical points $\rho(\mathbf{r}_c)$ (e Å^{-3}), Laplacian of the electron density at the bond critical point $\nabla^2\rho(\mathbf{r}_c)$ (e Å^{-5}), energy density at the bond critical point $H(\mathbf{r}_c)$ (Hartree Å^{-3}) and bond ellipticity ε_c. Values are taken from [14].
[b] Bond order according to Cioslowski and Mixon [37].
[c] Position of the bond critical point given by $d_c = (\mathbf{r}_c – C_{carbene})/(C_{carbene} – W)$.

Schrock-type tungsten complexes (Fig. 6) using various charge-partitioning methods. Although there is no strict definition of the two classes of compounds which is valid for all carbene complexes, chemical behaviour and structural characteristics may be used for a classification. The carbene ligand of Fischer complexes is usually electrophilic, while Schrock complexes have a nucleophilic center. Fischer complexes have transition metals which are usually in a low oxidation state, whereas typical Schrock complexes have transition metals in a high oxidation state. Fischer complexes can only become isolated when the carbene ligand is stabilized by a π-donor substituent, while Schrock complexes may have have carbene ligands CR_2 where R = hydrogen or alkyl group.

The focus of the theoretical work of VF was the search for characteristic differences in the electronic structure of the $L_nW–C_{carbene}$ bond. The authors employed the Bader analysis [21], the NBO [22] method and the CDA [17]. The Bader analysis has the advantage that the results are obtained from analyzing the topography of the total electron density which is experimentally observable. The results do not depend on a bonding model which depends on the definition of the interacting fragments like the CDA and EDA, nor does it depend on the description of the electronic structure in terms of the Lewis bonding model like the NBO partitioning scheme. This makes the Bader method particularly useful for analyzing the difference between the electronic structures of Fischer and Schrock carbenes.

Table 5 shows the results of the Bader analysis for the 12 carbene complexes **1**–**12** shown in Fig. 6. The contour line diagrams of the Laplacian of selected compounds are shown in Fig. 7. Visual inspection of the Laplacian shows clearly the difference between Fischer and Schrock complexes. There are hardly any changes at the carbene ligand when the contour line diagrams in the CH_2 plane are compared (Figs. 7(a), (e), (g), (i), and (k)). The area of charge concentration at the carbene carbon atom pointing towards the

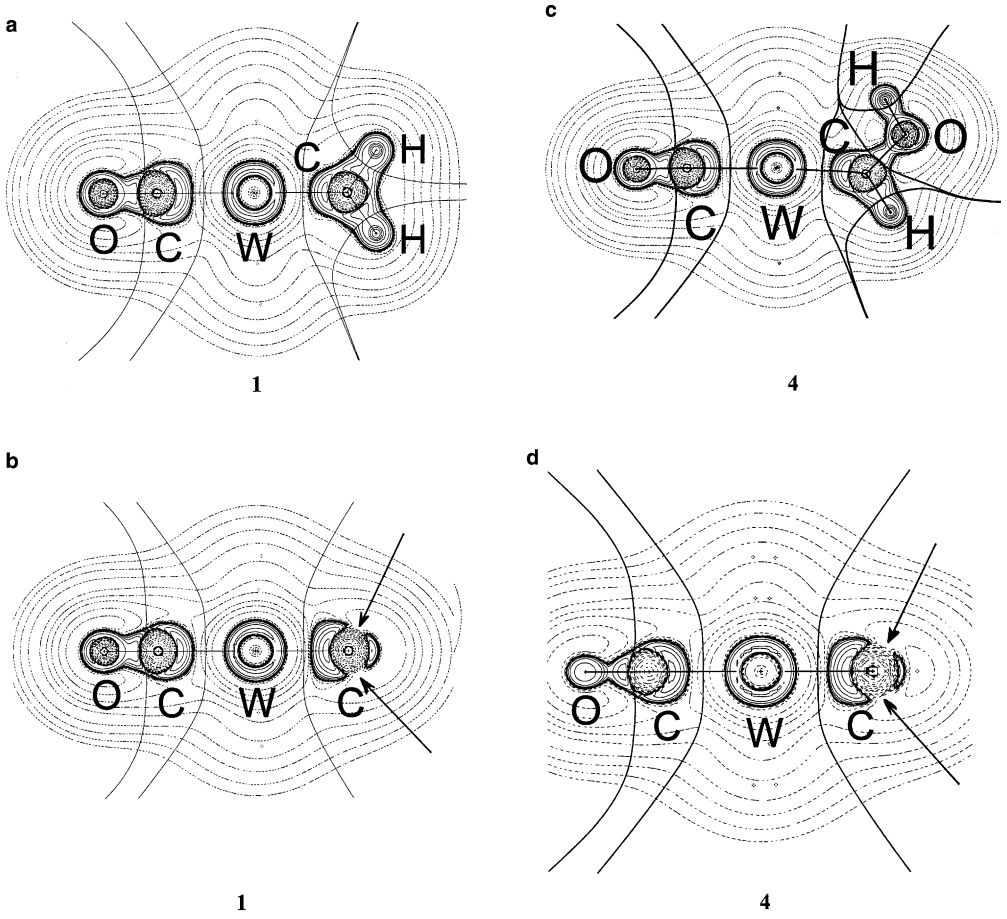

Fig. 7. Contour line diagrams of the Laplacian $\nabla^2\rho(\mathbf{r})$ at MP2/II of: (a) compound **1** in the plane of the carbene ligand; (b) compound **1** perpendicular to the plane of the carbene ligand; (c) compound **4** in the plane of the carbene ligand; (d) compound **4** perpendicular to the plane of the carbene ligand; (e) compound **5** in the plane of the carbene ligand; (f) compound **5** perpendicular to the plane of the carbene ligand; (g) compound **11** in the plane of the carbene ligand; (h) compound **11** perpendicular to the plane of the carbene ligand; (i) free ($^1A_1$) CH_2 in the molecular plane; (j) free ($^1A_1$) CH_2 perpendicular to the molecular plane; (k) free ($^3B_1$) CH_2 in the molecular plane; and (l) free ($^3B_1$) CH_2 perpendicular to the molecular plane. Solid lines indicate areas of charge concentration ($\nabla^2\rho(\mathbf{r}) < 0$) while dashed lines show areas of charge depletion ($\nabla^2\rho(\mathbf{r}) > 0$). The solid lines connecting the atomic nuclei are the bond paths; the solid lines separating the atomic nuclei indicate the zero-flux surfaces in the plane. The crossing points of the bond paths and zero-flux surfaces are the bond critical points $\mathbf{r}_c$. The large arrows in (b) and (d) show the hole in the valence sphere of the carbene ligand that is prone to attack by a nucleophilic agent. Reproduced with permission from [14].

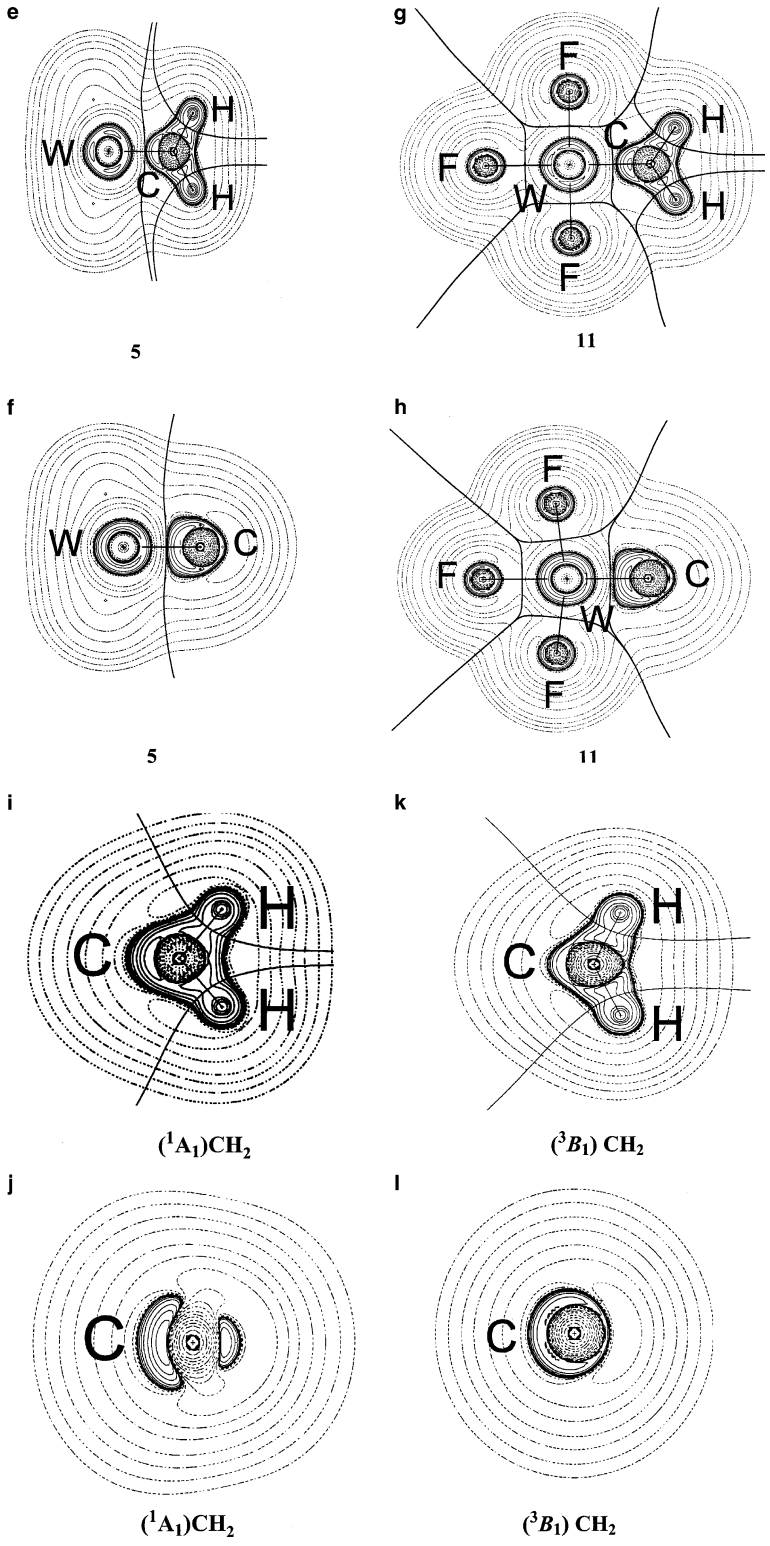

Fig. 7 (*continued*)

tungsten atom, which corresponds to the carbon lone-pair electrons of CH_2, is not much distorted by the presence of the metal fragment in both types of carbene ligands. Significant differences are found when the Laplacian in the π plane of the carbene ligand is examined. The parent Fischer complex **1** which has no π-donor substituent at the carbene ligand exhibits an area of charge depletion (dashed lines) in the direction of the p(π) orbitals of the carbene carbon atoms. This is indicated by the arrows in Fig. 7(b). The holes in the electron concentration are visible signs for the direction of a possible nucleophilic attack at the carbene ligand. They are still present in the π-donor substituted complex **4**

(Fig. 7(d)). In contrast to the Fischer complexes, the carbene carbon atoms of the Schrock complexes **5** and **11** are shielded by continuous ares of charge concentration (Figs. 7(f) and (h)). The carbene ligands of **5** and **11** have Laplacians which are similar to those of ($^3B_1$) CH_2, while the carbene ligand of **1** resembles ($^1A_1$) CH_2.

A closer examination of Fig. 7 shows that the position of the bond critical point $\mathbf{r}_c$ of the W–$C_{carbene}$ bond is, in case of the Schrock complexes **5** and **11**, closer to the charge concentration of the carbene carbon atoms compared with the Fischer complexes **1** and **4**. This is important, because the calculated values at the bond critical point can be used to classify the nature of the bond [21,66]. The calculated values indicate that the W–$C_{carbene}$ bonds of the Fischer complexes **1**–**4** exhibit significant differences from the Schrock complexes **5**–**12**. Firstly, the energy difference at the bond critical point $H(\mathbf{r}_c)$ has much larger negative values for **5**–**12** than for **1**–**4**. It has been shown that shared-electron (covalent) bonds have strongly negative energy values at the bond critical point, while closed-shell interactions (ionic bonds or van der Waals interactions) have $H(\mathbf{r}_c)$ values which are very small [66]. The $H(\mathbf{r}_c)$ values of the W–$C_{carbene}$ bonds of **1**–**4** are comparable in magnitude to the W–CO donor–acceptor bonds, while the W–$C_{carbene}$ bonds of **5**–**12**. have much more negative $H(\mathbf{r}_c)$ values not only in comparison to the W–$C_{carbene}$ bonds of **1**–**4** but also to the W–X bonds (X = halogen or oxygen) of **5**–**12**, thereby indicating a larger degree of covalent character.

A second distinctive property between the Fischer and Schrock carbenes are the calculated Cioslowski-Mixon bond orders. The Schrock complexes have bond orders for the W–$C_{carbene}$ bonds between 1.48 (for **11**) and 1.87 (for **9**), while the Fischer complexes have values between 0.93 (for **2** and **4**) and 1.18 (for **1**). Another useful quantity is the ellipticity at the bond critical point ε_c, which is sometimes viewed as a measure of the double-bond character [67]. The ε_c values show that the W–$C_{carbene}$ bonds of the Schrock complexes **5**–**12** have a much higher double-bond character than the Fischer complexes **1**–**4**. The value of the electron density $\rho(\mathbf{r}_c)$ and its Laplacian $\nabla^2\rho(\mathbf{r}_c)$ at the bond critical point is also clearly different for the Fischer and Schrock complexes. These results are in line with the DIs obtained for Fischer carbenes in the previous Section.

The NBO analysis gives further information about the W–$C_{carbene}$ bonds. The results are given in Table 6. The NBO data also exhibit typical differences between the Fischer and Schrock complexes. The optimal Lewis structure predicted by the NBO-partitioning scheme for the Fischer complexes **1** and **3** has a W–$C_{carbene}$ σ and π bond, while **2** and **4**, which are more realistic models for a Fischer complex, have only a σ bond. The W–$C_{carbene}$ σ bond of **1**–**4** is clearly polarized towards the carbon end (only 23–28% are at the tungsten end), while the W–$C_{carbene}$ π bond of **1** and **3** is polarized (63% and 67%) toward W. The NBO bonding pattern for **2** and **4** suggests that the W–$C_{carbene}$ π bond is even more polarized towards the metal moiety, because the optimal Lewis structure has a tungsten lone-pair d(π) orbital rather than a π bond. The calculated hybridization shows that the σ bond has mainly d character at the tungsten end, while the π bond at tungsten is purely d(W). The

Table 6
Results of the NBO analysis of the tungsten carbene complexes **1**–**12** at the MP2/II level[c]

	Atom			Occup.	W–C bond				W	Charge CXY[a]	p(π) Carbene[b]
	6s	5d	6p		%W	%s	%p	%d			
1	0.53	5.86	0.02	σ: 1.77	24.51	11.5	11.1	77.4	−0.41	−0.13	0.67
				π: 1.68	62.90	0	0	100			
2	0.50	6.06	0.02	σ: 1.91	28.19	31.6	0	68.4	−0.57	+0.04	0.67
3	0.49	5.97	0.02	σ: 1.77	22.66	10.3	16.3	73.4	−0.48	−0.04	0.67
				π: 1.66	67.27	0	0	100			
4	0.49	6.02	0.02	σ: 1.90	27.95	30.8	0	69.2	−0.54	+0.13	0.61
5	0.33	3.16	0.05	σ: 1.94	38.77	29.7	0	70.3	+2.41	−0.38	1.20
				π: 1.74	33.82	0	29.2	70.8			
6	0.37	3.22	0.07	σ: 1.94	34.75	29.3	0	70.7	+2.32	−0.33	1.13
				π: 1.73	39.33	0	21.5	78.5			
7	0.45	4.37	0.05	σ: 1.94	41.47	18.0	0	81.6	+1.06	−0.24	1.11
				π: 1.95	48.63	0	9.9	89.9			
8	0.50	4.72	0.07	σ: 1.94	41.10	19.5	0	80.5	+0.63	−0.24	1.10
				π: 1.80	42.43	0	21.4	78.6			
9	0.57	4.97	0.10	σ: 1.794	41.11	15.0	0	85.0	+0.27	−0.25	4.09
				π: 1.90	45.67	0	10.1	89.9			
10	0.36	3.46	0.04	σ: 1.77	30.13	21.7	5.80	72.5	+2.140	−0.40	1.17
				π: 1.68	33.27	0	29.0	71.0			
11	0.31	3.06	0.07	σ: 1.94	27.71	35.3	0	64.7	+2.45	−0.63	1.19
				π: 1.94	42.70	0	0	100			
12	0.32	3.16	0.07	σ: 1.93	24.38	35.0	0	65.0	+2.34	−0.54	1.12
				π: 1.75	40.85	0	0	0			

[a] Partial charge of the carbene ligand.
[b] Natural occupation of the 2p-π orbital of C.
[c] Values are taken from [14].

carbene ligand of the Fischer complexes carries only a small partial charge between −0.13 and +0.13.

The population of the p(π) AO of the CH_2 carbene carbon atom in **1** (0.67) is very similar to the values calculated for the CHF, CF_2, and CHOH ligands in **2**–**4** (Table 6). The NBO result is in agreement with the Laplacian of **1** and **4** in the π plane of the carbene ligands, which show holes in the electron concentration of both molecules. This is surprising, because **4** is experimentally a clearly more stable Fischer complex than **1**, which is usually explained with the stabilization of the p(π) orbital of the carbene carbon atom by the substituent. The NBO results suggest that the higher stability of **4** relative to **1** is a kinetic effect. Breaking the W–$C_{carbene}$ bond of **4** retains the electronic stabilization of the carbene ligand by donation of the OH substituent into the p(π) orbital, while the only stabilization of the carbene through metal → carbene π back-donation is lost when the W–$C_{carbene}$ bond of **1** is stretched. This makes the reaction of the carbene ligand of **1** with a nucleophilic agent more favorable compared with that of **4**.

The Schrock complexes **5**–**12** exhibit very different NBO results compared to those of the Fischer complexes **1**–**4**: (i) All Schrock complexes have W–$C_{carbene}$ σ and π bonds that are both polarized towards the carbon end. The calculated polarization of the π bond is in agreement with the previous study of Taylor and Hall [6], who found that the π electrons in Fischer complexes are polarized towards the metal, while in the Schrock complex they are more equally distributed. The d(W) AOs contribute the largest parts of the W–$C_{carbene}$ σ and π bonds at the tungsten end. Note that the polarization of the σ bonds of the neutral Schrock complexes **5**–**10** is very similar to that of the respective π bonds. (ii) The carbene ligands of **5**–**12** carry a distinct negative partial charge. (iii) The population of the p(π) orbital of the carbene carbon atoms is significantly higher (1.09–1.20) in the Schrock complexes than in the Fischer complexes. This explains why the Laplacian of the electron density in the Schrock complexes has an area of electron concentration around the carbene carbon atoms, while the Fischer complexes have a hole in the π direction. Thus, the NBO analyses of the **1**–**12** complement nicely the results of the topological analysis of the electron-density distribution. This is gratifying, because the NBO analysis focuses on the orbital structure of the molecules, while the topological analysis considers the total electron-density distribution.

Another difference between the Fischer complexes **1**–**4** and the Schrock complexes **5**–**12** concerns the electronic configuration and the atomic partial charge at the metal. The tungsten 5d-shell population in the Fischer complexes is ∼6 electrons, and the small negative partial charges ∼−0.5 are due to the population of the 6s orbital (Table 6). The calculated 5d population agrees with the formal notation of these compounds as W(6d) compounds with the oxidation state zero (i.e., W(0)). However, the concept of oxidation state is based on formal assignments of the bonding electrons to the metal and the ligand. The NBO results for the Schrock complexes show that the formal charge is as low as −0.27 for **9**. The calculated partial charges indicate that the tungsten atom of the Schrock complexes is more positively charged and has a lower 5d population than the Fischer complexes. Note that the negatively charged complexes **11** and **12** have practically the same partial charge at the metal as the respective neutral compounds **5** and **6**. This is because the fluorine atoms carry most of the additional charge.

The CDA results of **1**–**12** are given in Table 7. The results for the carbonyl ligand in $W(CO)_6$ is given for comparison. The data for the Fischer complexes **1**–**4** indicate that the carbene ligand is a stronger electron donor than electron acceptor. We want to emphasize that the *absolute* numbers of the carbene → metal donation and metal → carbene back-donation are not important, but rather the *relative* values. The donation/back-donation ratio for **1**–**4** suggests that the carbene ligands have the order of acceptor strength $CH_2 < CHF < CF_2 < CHOH$. The repulsive polarization term is always negative. This is reasonable, because it gives the amount of electronic charge that is removed from the overlapping area of occupied orbitals of the ligand and the metal fragment. The residue term is ∼0. This means that the complexes **1**–**4** can be reasonably interpreted as complexes between closed-shell fragments $W(CO)_5$ and CXY.

A comparison of the relative donor/acceptor ability of the CHOH ligand of **4**, which is a realistic model for a carbene ligand of a Fischer complex, and CO is very interesting. Fischer concluded from the observed C–O stretching frequencies of $(CO)_5CrL$ (where L = CO or $C(OCH_3)(Ph)$) that the carbene ligand possesses a substantially larger σ donor/π acceptor ratio than CO [68]. Table 7 shows that the CDA results are in agreement with Fischer's suggestion. The calculated σ donor/π acceptor ratio of CHOH in **4** is 0.417/0.177 = 2.36, the value for CO in $W(CO)_6$ is 0.315/0.233 = 1.35.

Table 7
CDA results for the carbene complexes **1**–**12** at the MP2/II level[a]

	Carbene → WL_n donation	L_nW → carbene back-donation	L_nW ↔ carbene repulsion	Residue term
1	0.314	0.282	−0.370	0.016
2	0.369	0.219	−0.289	0.027
3	0.324	0.268	−0.325	0.017
4	0.417	0.77	−0.285	0.032
5	0.013	−0.084	0.209	0.380
6	0.440	0.223	−0.311	0.351
7	−0.031	−0.058	0.141	0.416
8	−0.014	−0.074	0.113	0.406
9	0.343	−0.044	−0.271	0.423
10	0.016	−0.069	0.221	0.396
11	0.451	0.234	−0.334	−0.006
12	0.440	0.223	−0.311	0.005
$[W(CO)_6]$[b]	0.315	0.233	−0.278	

[a] Values are taken from [14].

[b] The values give the CO → $W(CO)_5$ donation, $W(CO)_5$ → CO back-donation and $W(CO)_5$ ↔ CO repulsive polarization.

The CDA results for the neutral Schrock complexes **5**–**10**, which are calculated from the interactions between closed-shell fragments WL_4 and the carbene ligand, differ substantially from the data of the Fischer complexes. The donation and back-donation terms are in some cases negative, which is a physically unreasonable result. More striking are the results for the residue term, which gives the contributions of the unoccupied orbitals of the fragments to the electronic structure of the respective complex. The residue terms have in all cases large positive numbers. This means that the electronic structure of **5**–**10** should not be discussed in terms of donor–acceptor interactions between the closed-shell carbene ligand and the metal fragment. Inspection of the orbitals that make up the residue term shows that the p(π) AO of the carbene carbon atom, which is unoccupied in the CH_2 fragment, is a large contributor to the metal–carbene interactions. This means that the W–$C_{carbene}$ bonds of **5**–**10** should be discussed in terms of interactions between the ($^3B_1$) triplet state of the carbene and the triplet ground state of WCl_4 as shown in Fig. 1(b). The CDA result for **5**–**10** support the bonding model suggested by Taylor and Hall [6] for Schrock complexes.

The CDA results for the negatively charged Schrock complexes **11** and **12** suggest that the metal–carbon bonding in these compounds can be interpreted as donor–acceptor interactions between the closed-shell fragments WCl_5^- and CX_2. This is not surprising, because WCl_5^- has a singlet ground state, while WCl_4 is a triplet. The values for the residue term of **11** and **12** are ~0. CH_2 and CF_2 are even better donor ligands in **11** and **12** than in **1** and **2** (Table 7). The CDA results for **11** and **12** show that a transition metal in a Schrock-type high oxidation state may have a donor–acceptor carbene bond just like a Fischer-type carbene complex, which has a metal in a low oxidation state. We want to point out that a similar situation exists for transition metal complexes with π-bonded ligands such as ethylene or acetylene. The analysis of the bonding situation in $W(CO)_5L$ complexes (L = ethylene, acetylene) with the CDA method showed that these compounds should be considered as donor–acceptor complexes, while WCl_4L compounds should be interpreted as metallacyclic molecules. The corresponding anions $[WCl_5L]^-$ are borderline cases which can be considered as both donor–acceptor complexes and electron-sharing compounds [34].

The CDA results may lead to the conclusion that the carbene → metal σ donation is clearly more important for the binding energy than the metal → carbene π back-donation. This conclusion is not necessarily correct. The relative amounts of charge donation do not always correlate with the corresponding attractive interactions. The carbene lone-pair orbital overlaps not only with empty metal orbitals, but also with occupied metal d orbitals, which leads to repulsive interactions. With other words, larger alterations in the space of the σ electronic charge than in the π charge may not be used as evidence for stronger attractive interactions of the σ electrons. The contribution of the carbene → metal donation and π back-donation to the orbital interaction as well as the Pauli repulsion and the electrostatic attraction will be discussed in the next section which gives the EDA results of Fischer and Schrock carbene complexes and heavier group-14 analogues.

5. Energy decomposition analysis of Fischer-type and Schrock-type carbene complexes and heavier group-14 analogues $L_nTM–ER_2$ (E = C, Si, Ge, Sn, Pb)

The previous section has shown that the distinction between Fischer- and Schrock-type carbenes which is based on experimental observations and intuitive bonding models is supported by quantum chemical charge-partitioning methods. Here, we discuss the results of the energy partitioning analysis of Fischer-type tungsten complexes $(CO)_5W–CH_2$, $(CO)_5W–C(OH)_2$, and the heavier group-14 analogues $(CO)_5W–E(OH)_2$ (E = Si, Pb) which have been presented by Lein et al. [13].

Table 8 gives the EDA results of the calculated Fischer-type complexes. The data show that the hydroxyl groups have a significant influence on the strength and on the nature of the W–CR_2 bonding interactions. The calculated

Table 8
Energy decomposition analysis (kcal/mol) of the Fischer complexes $(CO)_5W–CH_2$ and $(CO)_5W–E(OH)_2$ using the metal fragments $(CO)_5W$ and the ligands CH_2 and $E(OH)_2$ in the singlet state[c]

Term	$(CO)_5W–CH_2$	$(CO)_5W–C(OH)_2$	$(CO)_5W–Si(OH)_2$	$(CO)_5W–Ge(OH)_2$	$(CO)_5W–Sn(OH)_2$	$(CO)_5W–Pb(OH)_2$
ΔE_{int}	−93.8	−56.0	−49.3	−30.8	−27.2	−15.0
ΔE_{Pauli}	188.1	129.2	120.8	74.7	63.7	35.0
ΔE_{elstat}[a]	−172.4 (61.2%)	−124.7 (67.3%)	−103.9 (61.1%)	−56.7 (53.7%)	−48.6 (53.4%)	−20.9 (41.8%)
ΔE_{orb}[a]	−109.5 (38.8%)	−60.5 (32.7%)	−66.2 (38.9%)	−48.8 (46.3%)	−42.4 (46.6%)	−29.1 (58.2%)
A_1	−50.6	−39.6	−44.7	−33.8	−31.5	−22.1
A_2	−0.1	−0.4	−0.3	−0.1	−0.1	−0.1
B_1	−53.1	−14.2	−12.7	−9.8	−6.9	−4.6
B_2	−5.7	−6.3	−8.5	−5.1	−3.8	−2.4
ΔE_σ[b]	46.4%	66.1%	68.0%	69.5%	74.7%	76.1%
ΔE_π[b]	53.6%	33.9%	32.0%	30.5%	25.3%	23.9%

[a] The value in parentheses gives the percentage contribution to the total attractive interactions.
[b] The value in parentheses gives the percentage contribution to the total orbital interactions.
[c] Values are taken from [13].

Table 9
Energy decomposition analysis (kcal/mol) of the Schrock complexes $Cl_4W–EH_2$ using the fragments Cl_4W and EH_2 in the triplet state[c]

Term	$Cl_4W–CH_2$	$Cl_4W–SiH_2$	$Cl_4W–GeH_2$	$Cl_4W–SnH_2$	$Cl_4W–PbH_2$
ΔE_{int}	−132.5	−88.0	−83.3	−71.5	−65.3
ΔE_{Pauli}	260.7	156.3	150.2	129.1	120.1
ΔE_{elstat}[a]	−190.0 (48.3%)	−120.4 (49.3%)	−114.8 (49.2%)	−100.8 (50.2%)	−86.9 (46.9%)
ΔE_{orb}[a]	−203.2 (51.7%)	−123.9 (50.7%)	−118.6 (50.8%)	−99.9 (49.8%)	−98.5 (53.1%)
A_1	−129.7	−80.7	−79.1	−67.4	−64.2
A_2	−0.1	−0.1	−0.1	−0.1	−0.1
B_1	−12.7	−5.5	−5.4	−4.0	−4.4
B_2	−60.7	−37.5	−34.1	−28.4	−29.8
ΔE_σ[b]	63.9%	65.3%	66.7%	67.5%	65.2%
ΔE_π[b]	36.1%	34.7%	33.3%	32.5%	34.8%

[a] The value in parentheses gives the percentage contribution to the total attractive interactions.
[b] The value in parentheses gives the percentage contribution to the total orbital interactions.
[c] Values are taken from [13].

interaction energy in $(CO)_5W–C(OH)_2$ ($\Delta E_{int} = -56.0$ kcal/mol) is much less than in $(CO)_5W–CH_2$ ($\Delta E_{int} = -93.8$ kcal/mol). The same result was found for the chromium complex (Table 2) where the π-donor substituent weakens the metal–carbene bond dissociation energy (BDE). The bonding in the former compound is less covalent ($\Delta E_{orb} = 32.7\%$) than in the latter ($\Delta E_{orb} = 38.8\%$) but the $\pi_\perp$-contribution to the $(CO)_5W–C(OH)_2$ bonding is *much* less ($\Delta E_{\pi\perp} = 23.5\%$) than in $(CO)_5W–CH_2$ ($\Delta E_{\pi\perp} = 48.5\%$) [69]. This is striking evidence that the π-donor substituents OH have a strong influence on the nature of the metal–carbene interactions. The strength of the $(CO)_5W–E(OH)_2$ bonding interactions decreases while the covalent character increases when E becomes heavier (Table 8). The difference between the π character of the carbene complex and the silylene and germylene homologues is not very large.

Table 9 gives the EDA results of the Schrock complexes $Cl_4W–EH_2$ (E = C, Pb). The strength of the $Cl_4W–EH_2$ interactions is much higher than in the respective Fischer complexes $(CO)_5W–E(OH)_2$. The calculated ΔE_{int} value decreases when E becomes heavier but it remains rather high even for the lead complex $Cl_4W–PbH_2$ ($\Delta E_{int} = -65.3$ kcal/mol). Somewhat surprisingly, the nature of the W–E bonding in the Schrock carbenes changes very little for the different elements E. The $Cl_4W–EH_2$ bonds are half electrostatic and half covalent for all elements E. Two third of the covalent bonding comes from σ bonding and one third comes from $\pi_\perp$-bonding. Thus, the absolute values of the π contribution to ΔE_{cov} in the Schrock carbenes $Cl_4W–EH_2$ are much higher than in the respective Fischer complexes $(CO)_5W–E(OH)_2$ but the ratio of σ and $\pi_\perp$ bonding in the two classes of compounds is similar (Table 8).

6. Charge decomposition analysis of transition metal complexes with N-heterocyclic carbene ligands

The above discussion of Fischer-type complexes has shown that the metal → carbene π back-donation significantly contributes to the binding interactions. The carbene ligands in the complexes, which are discussed above, are not stable as free species in a condensed phase. There is a special class of transition metal donor–acceptor carbene complexes where the π-bonding contribution to the metal–carbene bonding appears to be less important or even negligible. These are complexes of N-heterocyclic carbenes (NHCs) like imidazol-2-ylidene and related compounds which can be isolated as free molecules [9]. The nature of the bonding and in particular the question of the π-bonding contribution in typical NHC-complexes was the subject of two theoretical studies of our groups. One study by Boehme and Frenking [16] reported about an electronic structure analysis of group-11 (Cu, Ag, Au) complexes ClTM–NHE with E = C, Si, Ge where NHC is the parent imidazol-2-ylidene ligand and NHSi and NHGe are the silicon and germanium analogues. The authors used the CDA, NBO and Bader methods for the bonding analysis. The second study by Nemcsok et al. [15] analyzed the energetic aspects of the bonding interactions in the group-11 carbene complexes XAg–NHC, ClTM–NHC and $TM(NHC)_2^+$ where X = F, Cl, Br, I and TM = Cu, Ag, Au. The information about the bonding situation in the complexes which was gained in the two studies will be summarized in this and the following section.

We first discuss the results of the electronic structure analysis of Boehme and Frenking [16]. Fig. 8 shows the calculated geometries of the molecules ClTM–NHE and the free fragments because they are relevant for the bonding discussion. The calculations were performed at the MP2 level using valence DZP-quality basis sets. The most important point is, that the N–E bond lengths of the free ligands NHE become shorter in the complexes. Table 10 gives the CDA results of the compounds and the theoretically predicted bond dissociation energies.

The CDA results for the carbene compounds ClTM–NHC given in Table 10 support the suggestion that the metal → carbene π back-donation in NHC complexes is much smaller than the carbene → metal σ donation. The d/b ratio is clearly higher than in typical Fischer complexes (Table 1). The somewhat lower d/b ratio of the gold complex ClAu–NHC indicates some metal → carbene π

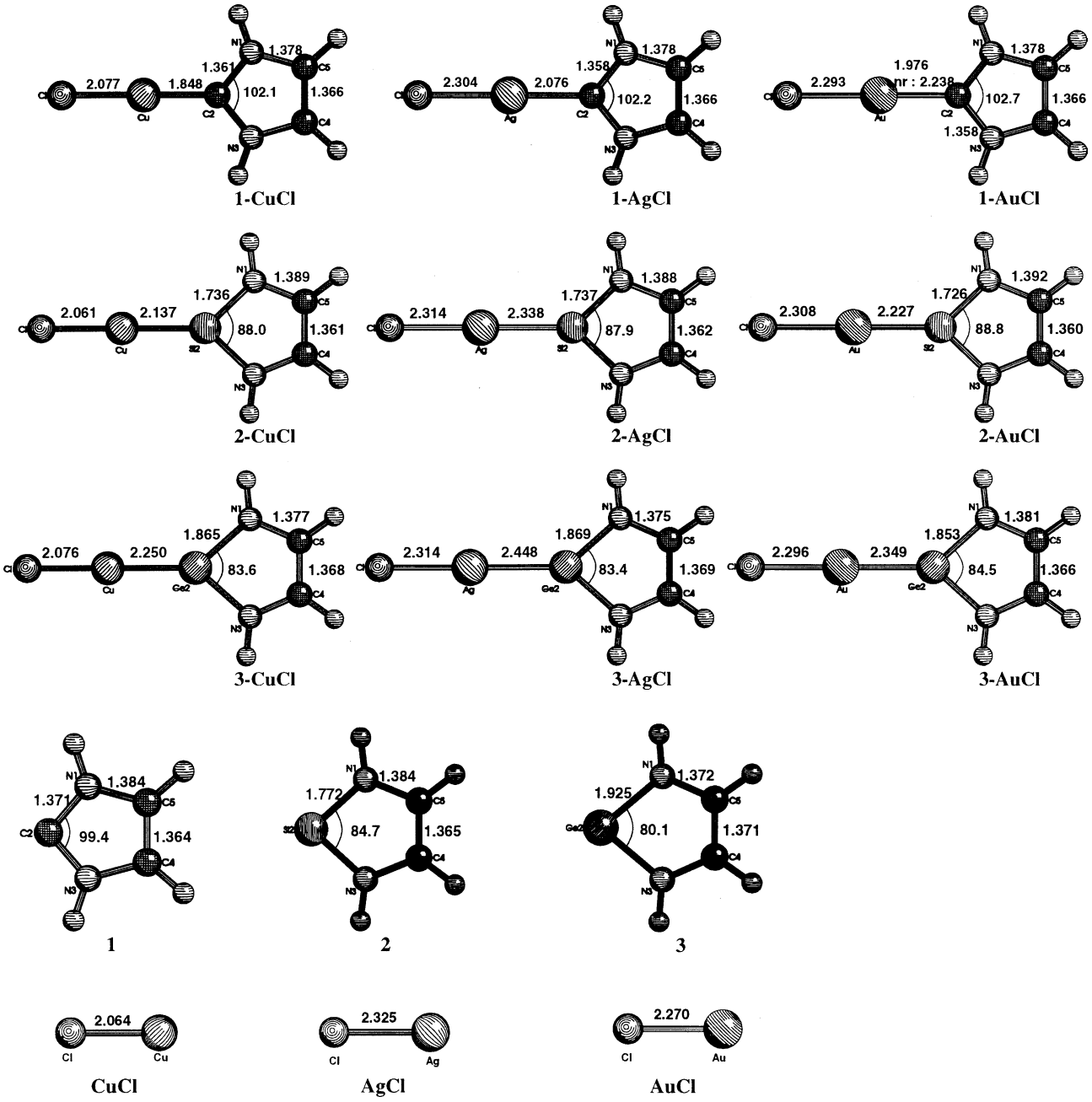

Fig. 8. Optimized geometries of the complexes ClTM–NHE and the free fragments. Bond lengths are given in Å, angles in degree. Reproduced with permission from [16].

back-donation which can be explained with the effect of relativity, which leads to a contraction of the s and p orbitals but to more diffuse d and f orbitals [70]. It is known that relativistic effects are particularly strong in gold compounds [70,71]. We want to point out that the carbene ligands have rather large bond dissociation energies which are predicted at the CCSD(T) level between 56.5 kcal/mol for ClAg–NHC and 82.8 kcal/mol for ClAu–NHC. The BDE values given in Table 10 and in Table 1 clearly show that there is no correlation between the strength of metal → carbene π back-donation and bond strength. The data in Table 10 also show that the silylene and germylene ligands in ClTM–NHSi and ClTM–NHGe have weaker bonds than the carbene ligands, but the calculated values for the BDE indicate that the metal–silylene and metal–germylene bonds are still quite strong. The metal → ligand π back-donation in the latter species is rather small as it is the case in the carbene ligands.

The results of the NBO analysis of the complexes ClTM–NHE which are shown in Table 11 nicely complement the CDA data. The atomic partial charges q(TMCl) indicate that the ligand NHE donates electronic charge to the TMCl acceptor fragment with the order NHC < NHGe < ClTM–NHSi. Please note that the donor

Table 10
Results of the CDA calculations of the compounds ClTM–NHE at MP2/DZP: NHE → TMCl donation d, NHE ← TMCl back-donation b, ratio d/b, and NHE ↔ TMCl repulsive polarization r[a]

Molecule	d	b	d/b	r	D_e
$ClCu–C_3H_4N_2$	0.538	0.081	6.64	−0.128	67.4
$ClAg–C_3H_4N_2$	0.446	0.046	9.70	−0.131	56.5
$ClAu–C_3H_4N_2$	0.396	0.091	4.35	−0.273	82.8
$ClCu–SiC_2H_4N_2$	0.740	0.156	4.74	−0.114	45.1
$ClAg–SiC_2H_4N_2$	0.714	0.162	4.41	−0.053	37.4
$ClAu–SiC_2H_4N_2$	0.622	0.286	2.17	−0.066	64.1
$ClCu–GeC_2H_4N_2$	0.693	0.106	6.54	−0.100	35.1
$ClAg–GeC_2H_4N_2$	0.490	0.094	5.21	−0.059	29.9
$ClAu–GeC_2H_4N_2$	0.527	0.168	3.14	−0.126	49.4

Calculated bond dissociation energies D_e (kcal/mol) at CCSD(T)/DZP//MP2/DZP.
[a] Values are taken from [16].

Table 11
Results of the NBO partitioning scheme of the compounds ClTM–NHE at MP2/DZP: population of the π-symmetric p orbital of atom E (E = C, Si, Ge) p_π(E), charges of atom E q(E), of TM q(TM) and of the TMCl fragment q(TMCl), and Wiberg bond indices P(M–E) and P(E–N)[a]

Molecule	p_π (E)	q (E)	q (TM)	q (TMCl)	P (TM–E)	P (E–N)
$ClCu–C_3H_4N_2$	0.84	−0.02	0.54	−0.16	0.451	1.206
$ClAg–C_3H_4N_2$	0.83	−0.01	0.54	−0.18	0.405	1.218
$ClAu–C_3H_4N_2$	0.86	0.04	0.38	−0.24	0.591	1.202
$ClCu–SiC_2H_4N_2$	0.59	1.00	0.48	−0.23	0.612	0.780
$ClAg–SiC_2H_4N_2$	0.60	0.98	0.50	−0.22	0.513	0.788
$ClAu–SiC_2H_4N_2$	0.59	1.11	0.32	−0.33	0.762	0.775
$ClCu–GeC_2H_4N_2$	0.65	0.88	0.49	−0.21	0.489	0.790
$ClAg–GeC_2H_4N_2$	0.67	0.84	0.53	−0.19	0.410	0.794
$ClAu–GeC_2H_4N_2$	0.64	0.98	0.32	−0.30	0.620	0.788
$C_3H_4N_2$	0.67	0.06				1.120
$SiC_2H_4N_2$	0.54	0.87				0.747
$GeC_2H_4N_2$	0.63	0.78				0.744
CuCl			0.71			
AgCl			0.74			
AuCl			0.54			

[a] Values are taken from [16].

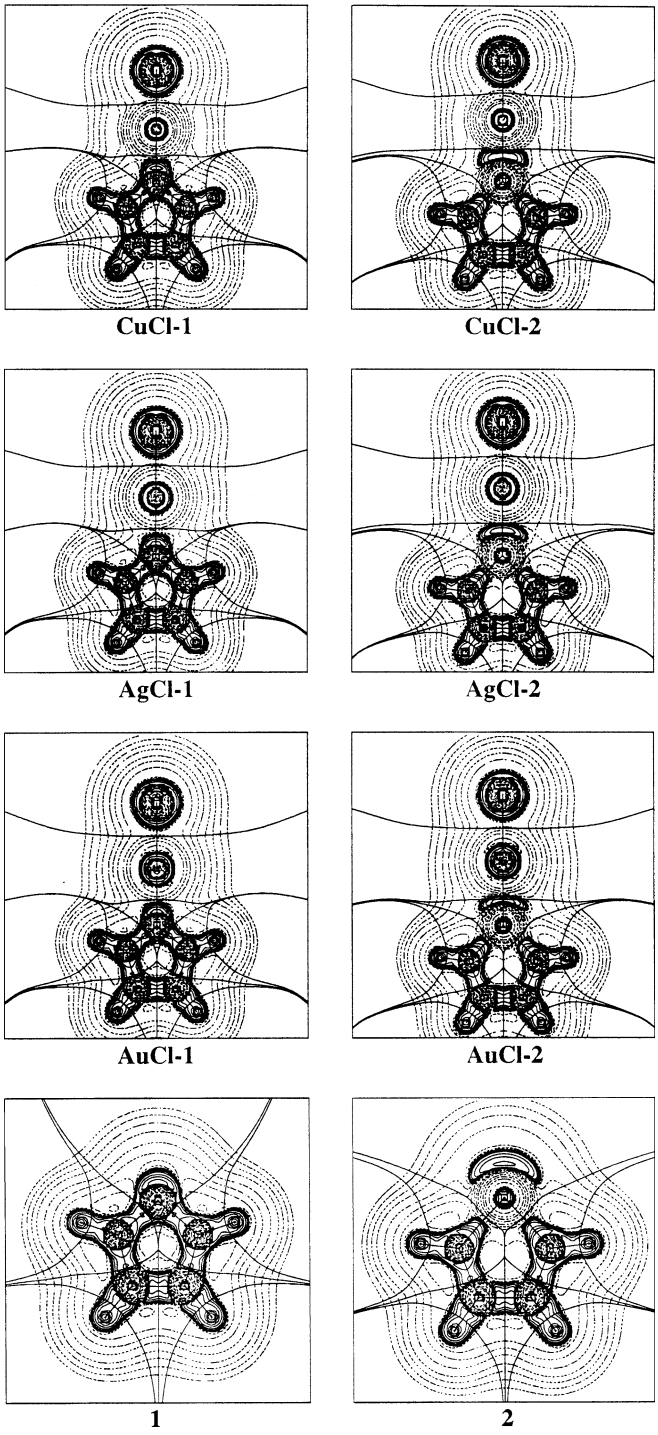

Fig. 9. Contour line diagrams of the Laplacian $\nabla^2\rho(\mathbf{r})$ at MP2/II of the complexes ClTM–NHE and the free ligands NHE (E = C, Si). Solid lines indicate areas of charge concentration ($\nabla^2\rho(\mathbf{r}) < 0$) while dashed lines show areas of charge depletion ($\nabla^2\rho(\mathbf{r}) > 0$). The solid lines connecting the atomic nuclei are the bond paths; the solid lines separating the atomic nuclei indicate the zero-flux surfaces in the plane. The crossing points of the bond paths and zero-flux surfaces are the bond critical points $\mathbf{r}_c$. Reproduced with permission from [16].

atom carbon which carries a slightly positive charge of 0.06 e in the free ligand NHC *receives* electronic charge although the NHC ligand is an overall donor, while the ligand atoms Si and Ge which are are strongly positively charged in NHE release electronic charge. More important than the overall charges are the alterations in the π distribution. Table 11 shows that the p(π) population of the donor atoms E is enhanced in the complexes compared to the free ligands. The increase is particularly strong in the carbene ligands but less so in the silylene and germylene complexes. But it is important to recognize that that the additional p(π) charge is not due to ClTM → E back-donation, but rather to stronger N → E π donation in the ligands. This becomes obvious from the calculated bond orders for the E–N bond, which are higher in the complexes than in the free ligands. The NHE → TMCl σ donation causes the donor atoms E to be come more electron deficient, which in turn induces stronger N → E π donation. This explains the shortening of the E–N bonds in the complexes. Further proof that the E–N bond shortening is an indirect effect of the E → MCl σ donation comes

Table 12
Results of the topological analysis of the electron density distribution of the compounds ClTM–NHE at MP2/DZP: electron density at the bond critical point ρ_c (Å^{-3}), Laplacian of the electron density at the bond critical point $\nabla^2\rho_c$ (Å^{-5}), and energy density at the bond critical point H_c (a.u./Å^3)[a]

Molecule	ρ_c			$\nabla^2\rho_c$			H_c		
	M–Cl	M–E	E–N	M–Cl	M–E	E–N	M–Cl	M–E	E–N
ClCu–$C_3H_4N_2$	0.688	0.882	2.100	9.368	11.076	−14.283	−0.185	−0.338	−3.461
ClAg–$C_3H_4N_2$	0.564	0.713	2.111	6.500	7.914	−13.611	−0.137	−0.236	−3.492
ClAu–$C_3H_4N_2$	0.652	1.000	2.128	6.173	7.900	−15.329	−0.207	−0.497	−3.524
ClCu–$SiC_2H_4N_2$	0.687	0.627	0.797	9.337	1.482	16.906	−0.182	−0.282	−0.254
ClAg–$SiC_2H_4N_2$	0.547	0.552	0.796	6.512	0.942	16.891	−0.124	−0.236	−0.254
ClAu–$SiC_2H_4N_2$	0.624	0.732	0.815	6.224	−2.657	17.397	−0.182	−0.500	−0.265
$C_3H_4N_2$			1.997			−9.106			−3.247
$SiC_2H_4N_2$			0.729			14.795			−0.222

[a] Values are taken from [16].

Table 13
Results of the NICS calculations at RHF/TZ[a]

Molecule	NICS
ClCu–$C_3H_4N_2$	−14.2
ClCu–$SiC_2H_4N_2$	−10.4
ClCu–$GeC_2H_4N_2$	−11.3
$C_3H_4N_2$	−13.7
$SiC_3H_4N_2$	−10.2
$C_3H_4N_2$	−10.8

[a] Values are taken from [16].

from the change when a proton is attached to the carbene carbon atom of NHC. Calculation at the MP2/6-31G(d) level show that the N–$C_{carbene}$ bond length in $(NHC)H^+$ is 0.032 Å shorter than in NHC [72].

The results of the topological analysis of the electron density distribution of the carbene and silylene complexes ClTM–NHE are shown in Fig. 9 and Table 12. Fig. 9 shows that the areas of charge concentration ($\nabla^2\rho(\mathbf{r}) < 0$, solid lines) at the donor atoms pointing toward the metal atoms which indicate the donor electron pair, are somewhat distorted in the complexes as result of the complex formation. Visual inspection of Fig. 9 shows that the distortion is less pronounced in the silver complexes than in the copper and gold complexes. This indicates that the Ag compounds may have a more electrostatic (ionic) metal–ligand bond than the Cu and Au compounds. This is supported by the calculated values of the energy density at the bond critical points for the metal–ligand bonds (Table 12). The H_c values for the ClAg–NHE bonds are less negative than those for the copper and gold analogues. A more detailed investigation of the covalent and electrostatic (ionic) character of the bond comes from the EDA calculations which are presented further below.

An interesting question concerns the aromatic character of the 6π systems NHE as free molecules and as ligands in the complexes ClTM–NHE. NMR chemical spectra of the bis(carbene) complexes $TM(NHC)_2^+$ (TM = Cu, Ag) with *N*-mesityl groups as substituents showed a substantial downfield shift for the imidazol ring protons compared to those of the free ligands, which may be interpreted in terms of higher degree of delocalization in the complexed imidazole rings [73]. Boehme and Frenking [16] performed nucleus-independent chemical shift (NICS) calculations which have been proven as sensitive probes of the aromatic character of a molecule [74]. Table 13 shows the calculated NICS values of the copper complexes ClCu–NHE and the free ligands NHE which were calculated at the center of the ring. The latter values may be compared with the calculated value of the free cyclopentadienyl anion $C_5H_5^-$ (−14.3 ppm), which may serve as a reference for a five-membered aromatic compound [74]. The data in Table 13 indicate that the free ligands NHE have a significantly aromatic character which becomes slightly enhanced in the complexes ClCu–NHE.

7. Energy decomposition analysis of transition metal complexes with N-heterocyclic carbene ligands

We summarize the most important results of the study by Nemcsok, Wichmann and Frenking [15] who analyzed the energetic aspects of the bonding interactions in the group-11 carbene complexes XAg–NHC, ClTM–NHC and $TM(NHC)_2^+$ where X = F, Cl, Br, I and TM = Cu, Ag, Au with the EDA method. Fig. 10 shows the optimized geometries of the complexes and the free carbene ligand and metal moieties and the bond dissociation energies of the carbene ligands at the BP86/TZ2P level. The authors investigated two structural isomers of $TM(NHC)_2^+$, one with perpendicular arrangement of the carbene rings, and the other one with coplanar arrangement of the rings. The structures with perpendicular carbene rings are minima on the potential energy surfaces, while the planar structures are marginally higher in energy ($\Delta E \leqslant 0.5$ kcal/mol) having one imaginary frequency with very small absolute values. The small energy differences between the planar and perpendicular structures could be taken as evidence that the π-contribution to the metal–ligand bonding is negligible. The energy decompositions analysis which is given below shows that this assumption is not justified.

A comparison of the geometries of ClTM–NHC which are predicted at BP86/TZ2P and MP2/DZP (Fig. 8) shows a rather good agreement between the two levels of theory. Note that the geometry of the carbene ring changes only

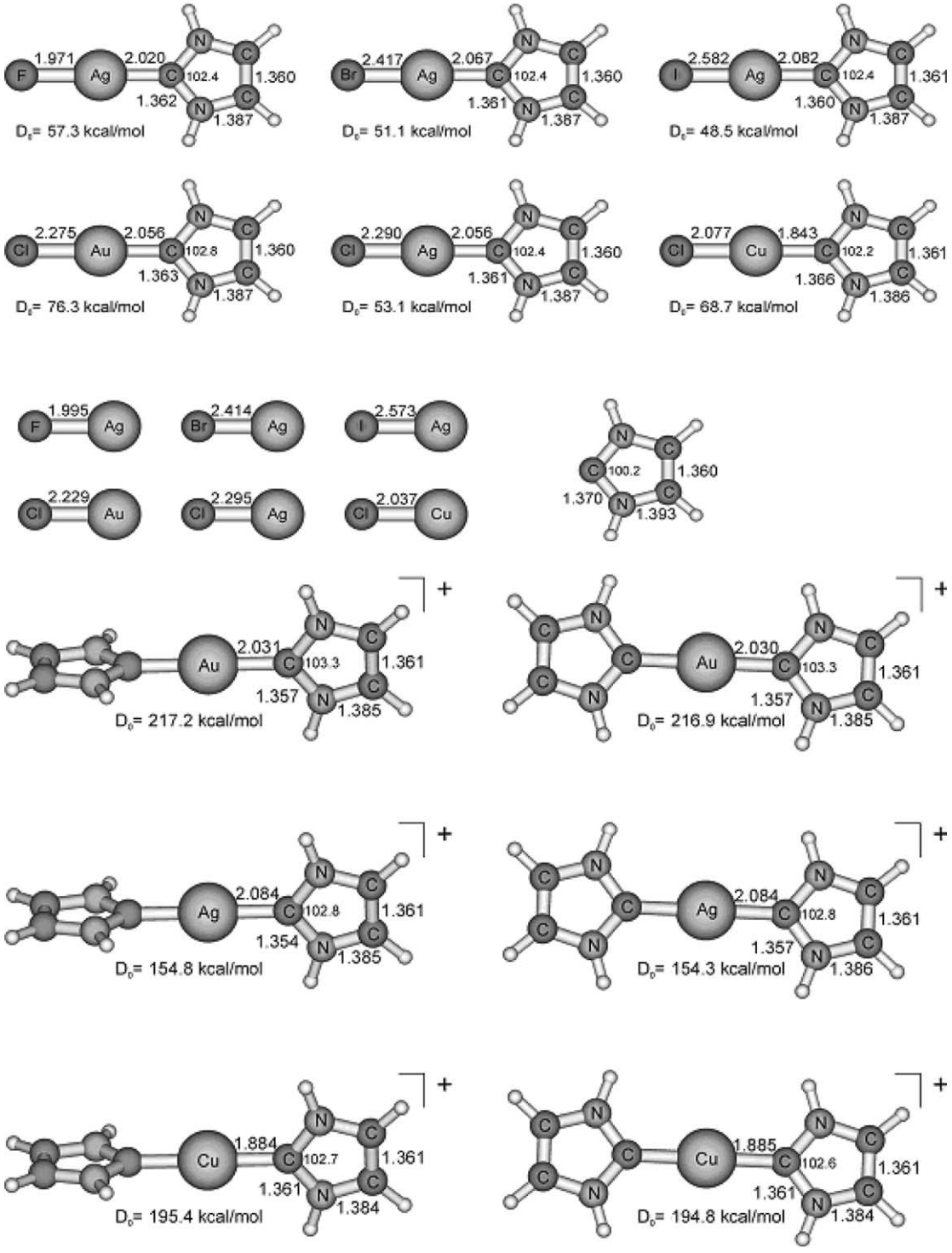

Fig. 10. Optimized geometries and dissociation energies of XAg–NHC, ClTM–NHC and $TM(NHC)_2^+$ (X = F, Cl, Br, I; TM = Cu, Ag, Au) at BP86/TZ2P. Bond lengths are given in Å, angles in °, energies in kcal/mol. The D_0 values refer to dissociation of one NHC ligand from XAg–NHC (top) and from two NHC ligands from $TM(NHC)_2^+$ (bottom). Reproduced with permission from [15].

slightly upon binding to the metal. The theoretically predicted BDE values at BP86/TZ2P (D_e values are given in Table 14) agree also remarkably well with the CCSD(T)/DZP values which are given in Table 10.

Table 14 gives the results of the EDA calculations of the XAg–NHC and ClTM–NHC (X = F, I; TM = Cu, Ag, Au) complexes. The largest contributions to the ΔE_{int} values come always from the electrostatic interaction term ΔE_{elstat} which contributes >75% to the binding energy while the orbital term contributes <25%. Note that the absolute value of ΔE_{elstat} for the silver complex ClAg–NHC is smaller than the values for the copper and gold

Table 14
Energy decomposition analysis of the mixed carbene halogen complexes XAg–NHC and ClTM–NHC (X = F, I; TM = Cu, Ag, Au) at BP86/TZ2P using the carbene ligand NHC and TMX as fragments[c]

	FAg–NHC	ClAg–NHC	BrAg–NHC	IAg–NHC	ClCu–NHC	ClAu–NHC
Symmetry	C_{2v}	C_{2v}	C_{2v}	C_{2v}	C_{2v}	C_{2v}
ΔE_{int}	−57.9	−53.6	−51.7	−49.0	−69.5	−77.5
ΔE_{Pauli}	138.0	127.9	125.7	123.8	126.7	211.3
ΔE_{elstat}[a]	−153.1 (78.2%)	−141.7 (78.1%)	−138.2 (77.9%)	−134.2 (77.7%)	−150.0 (76.4%)	−218.6 (75.7%)
ΔE_{orb}[a]	−42.8 (21.8%)	−39.3 (21.9%)	−39.2 (22.1%)	−38.6 (22.3%)	−46.2 (23.6%)	−70.2 (24.3%)
ΔE_{a1}[b]	−29.8 (69.6%)	−28.6 (71.9%)	−28.5 (72.8%)	−28.7 (74.3%)	−28.7 (62.0%)	−5.2 (71.5%)
ΔE_{a2}[b]	−0.2 (0.5%)	−0.2 (0.6%)	−0.2 (0.6%)	−0.2 (0.6%)	−0.1 (0.2%)	−0.3 (0.4%)
ΔE_{b1}[b]	−4.2 (9.7%)	−3.6 (9.0%)	−3.4 (8.8%)	−3.2 (8.3%)	−5.2 (11.2%)	−6.5 (9.3%)
ΔE_{b2}[b]	−8.6 (20.1%)	−7.3 (18.4%)	−7.0 (17.8%)	−6.5 (16.8%)	−12.3 (26.6%)	−13.2 (18.8%)
ΔE_{σ}[b]	−29.8 (69.6%)	−28.6 (71.9%)	−28.5 (72.8%)	−28.7 (74.3%)	−28.7 (62.0%)	−5.2 (71.5%)
$\Delta E_{\pi(\parallel)}$[b]	−4.2 (9.7%)	−3.6 (9.0%)	−3.4 (8.8%)	−3.2 (8.3%)	−5.2 (11.2%)	−6.5 (9.3%)
$\Delta E_{\pi(\perp)}$[b]	−8.6 (20.1%)	−7.3 (18.4%)	−7.0 (17.8%)	−6.5 (16.8%)	−12.3 (26.6%)	−13.2 (18.8%)
ΔE_{prep}	0.6	0.5	0.6	0.5	0.8	1.2
$\Delta E(-D_e)$	−57.3	−53.1	−51.1	−48.5	−68.7	−76.3
$-D_o$	−55.4	−51.4	−49.5	−47.0	−66.9	−74.5

Energies are given in kcal/mol.
[a] Values in parentheses give the percentage of the total attractive interactions $\Delta E_{elstat} + \Delta E_{orb}$.
[b] Values in parentheses give the percentage of the total orbital interactions ΔE_{orb}.
[c] Values are taken from [15].

complexes which is in agreement with the results of the AIM analysis given in the previous section. The strength of the interactions in the XAg–NHC complexes decreases with the order F > Cl > Br > I. The effect of the metal on the EDA results for the TM-carbene bond is larger than the effect of the halogen ligand. Note that the absolute values of ΔE_{Pauli}, ΔE_{elstat} and ΔE_{orb} of the gold complex are much larger than for the copper and silver homologues.

The C_{2v} molecular symmetry of the complexes XTM–NHC yields orbitals which belong to a_1, a_2, b_1, and b_2 irreducible representations. With our choice of the mirror planes, b_2 orbitals are in-plane $\pi_\parallel$ orbitals and b_1 orbitals are out-of-plane $\pi_\perp$ orbitals. The a_2 representation corresponds to δ orbitals. The a_1 orbitals have mainly σ symmetry, although there are a few orbitals of δ symmetry because the mirror planes of the orbital symmetry and the point group of the molecular symmetry do not always coincide. Assuming that the energy contribution from the a_1 (δ) orbitals is very small – of the same magnitude as the energy contribution from the a_2 orbitals – one can assign σ, in-plane $\pi_\parallel$, and out-of-plane $\pi_\perp$ energy contributions to the orbital symmetry. The total σ, $\pi_\parallel$, and $\pi_\perp$ contributions to the orbital interaction are listed in Table 14. By far the largest contributions come as expected from σ orbitals, and the in-plane $\pi_\parallel$ contributions account for one third of the total π interaction. The out-of-plane $\pi_\perp$ energy contributions constitute ⩽20% of the orbital interaction energy in the silver and gold complexes. The latter term is slightly larger in case of ClCu–NHC where the $\pi_\perp$ interactions contribute 26.6% to the orbital interactions. Given that the total orbital interaction accounts only for 22–25% of the attractive interaction, this is a rather small contribution, although it is not negligible compared to the σ interaction.

For the EDA calculations of the perpendicular equilibrium structures of $TM(NHC)_2^+$ two fragmentation schemes were employed. First, the bonding between one carbene ligand and the metal fragment $TM(NHC)^+$ was analyzed in order to allow for a comparison with the ClTM–NHC complexes. Then the bonding between two carbene ligands and a TM^+ cation was calculated with the EDA method in order to investigate the total σ- and π-bonding more closely. The second fragmentation scheme was also used for the planar structure of the bis(carbene) complexes. The results of the EDA calculations for the dissociation of one carbene ligand are shown in Table 15.

Table 15
Energy decomposition analysis of the bis(carbene) complexes $(\mathbf{1})_2TM^+$ (perpendicular structure) at BP86/TZ2P using one carbene ligand **1** and $(\mathbf{1})TM^+$ as fragments[c]

	$(\mathbf{1})_2Cu^+$	$(\mathbf{1})_2Ag^+$	$(\mathbf{1})_2Au^+$
Symmetry	D_{2d}	D_{2d}	D_{2d}
ΔE_{int}	−83.7	−70.1	−91.0
ΔE_{Pauli}	111.9	114.7	175.6
ΔE_{elstat}[a]	−146.2 (74.7%)	−140.5 (76.0%)	−197.7 (74.1%)
ΔE_{orb}[a]	−49.5 (25.3%)	−44.3 (24.0%)	−68.9 (25.9%)
ΔE_{a1}[b]	−33.0 (66.7%)	−32.1 (72.5%)	−51.3 (74.4%)
ΔE_{a2}[b]	−0.6 (1.3%)	−0.7 (1.6%)	−0.8 (1.1%)
ΔE_{a1}[b]	−5.0 (10.2%)	−7.7 (17.3%)	−11.1 (16.1%)
ΔE_{a2}[b]	−10.8 (21.8%)	−3.8 (8.6%)	−5.8 (8.4%)
ΔE_{σ}[b]	−33.0 (66.7%)	−32.1 (72.5%)	−51.3 (74.4%)
$\Delta E_{\pi(\parallel)}$[b]	−5.0 (10.2%)	−3.8 (8.6%)	−5.8 (8.4%)
$\Delta E_{\pi(\perp)}$[b]	−10.8 (21.8%)	−7.7 (17.3%)	−11.1 (16.1%)
ΔE_{prep}	1.3	0.9	2.5
$\Delta E(-D_e)$	−82.4	−69.2	−88.5
$-D_o$	−80.3	−67.0	−86.5

Energies are given in kcal/mol.
[a] Values in parentheses give the percentage of the total attractive interactions $\Delta E_{elstat} + \Delta E_{orb}$.
[b] Values in parentheses give the percentage of the total orbital interactions ΔE_{orb}.
[c] Values are taken from [15].

The EDA data in Table 15 show that the strength of the metal–carbene interactions and the dissociation energies of NHC–TM(NHC)$^+$ are larger than for NHC–TMCl. This can be explained with the positively charged metal fragment in the former species. The proportion of orbital interactions to the total attractive interaction in the former compounds varies from 24.0% to 25.9% and is thus only marginally higher than in the NHC–TMCl compounds. The molecular symmetry of the perpendicular structure of TM(NHC)$_2^+$ is D_{2d}, but for the EDA calculations the symmetry is reduced to C_{2v} because the fragment with the lowest symmetry determines the overall symmetry. Thus, the orbital interaction can be split up into contributions of σ, in-plane ($\pi_\parallel$) and out-of-plane ($\pi_\perp$) symmetry, similar to the NHC–TMCl compounds. A schematic representation of the $\pi_\parallel$ and $\pi_\perp$ orbitals is shown in Fig. 11. Table 15 shows that the copper complex Cu(NHC)$_2^+$ has the highest relative amount of out-of-plane $\pi_\perp$ interaction (21.8%). In the silver and gold complexes, the out-of-plane $\pi_\perp$ orbitals contribute only 17.3% and 16.1% to the orbital interaction term, respectively.

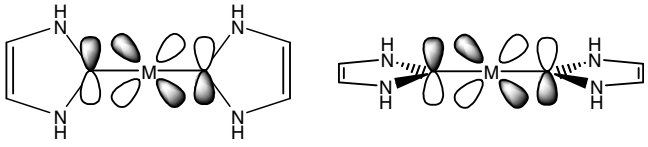

Fig. 11. Schematic representation of the in-plane ($\pi_\parallel$) and out-of-plane ($\pi_\perp$) π-orbital interactions in TM(NHC)$_2^+$.

Table 16
Energy decomposition analysis of the bis(carbene) complexes (**1**)$_2$TM$^+$ (perpendicular structure) at BP86/TZ2P using one carbene ligand **1** and (**1**)TM$^+$ as fragments[d]

	(**1**)$_2$Cu$^+$	(**1**)$_2$Ag$^+$	(**1**)$_2$Au$^+$
Symmetry	D_{2d}	D_{2d}	D_{2d}
ΔE_{int}	−203.8	−161.3	−224.8
ΔE_{Pauli}	219.9	226.4	348.8
ΔE_{elstat}[a]	−290.0 (68.4%)	−274.4 (70.8%)	−389.4 (67.9%)
ΔE_{orb}[a]	−133.7 (31.6%)	−113.4 (29.2%)	−184.2 (32.1%)
ΔE_{a1}[b]	−71.8 (53.7%)	−66.4 (58.5%)	−122.0 (66.2%)
ΔE_{a2}[b]	−1.0 (0.7%)	−0.9 (0.7%)	−0.9 (0.5%)
ΔE_{b1}[b]	−0.9 (0.7%)	−1.4 (1.3%)	−1.8 (1.0%)
ΔE_{b2}[b]	−20.4 (15.3%)	−16.3 (14.3%)	−19.9 (10.8%)
ΔE_{e}[b]	−39.6 (29.6%)	−28.5 (25.1%)	−39.6 (21.5%)
ΔE_{σ}[b]	−92.3 (69.0%)	−82.6 (72.9%)	−141.9 (77.0%)
ΔE_{π}[b]	−39.6 (29.6%)	−28.5 (25.1%)	−39.6 (21.5%)
ΔE_{prep}	8.4	6.5	7.6
$\Delta E(-D_e)$[c]	−195.4	−154.8	−217.2
$-D_o$[c]	−191.4	−151.2	−213.3

Energies are given in kcal/mol.
[a] Values in parentheses give the percentage of the total attractive interactions $\Delta E_{elstat} + \Delta E_{orb}$.
[b] Values in parentheses give the percentage of the total orbital interactions ΔE_{orb}.
[c] The dissociation energy refers to the reaction (**1**)$_2$TM$^+ \rightarrow$ TM$^+ + 2$ **1**.
[d] Values are taken from [15].

Table 17
Energy decomposition analysis of the bis(carbene) complexes (**1**)$_2$TM$^+$ (planar structure) at BP86/TZ2P using two carbene ligands (**1**)$_2$ and TM$^+$ as fragments[d]

	(**1**)$_2$Cu$^+$	(**1**)$_2$Ag$^+$	(**1**)$_2$Au$^+$
Symmetry	D_{2h}	D_{2h}	D_{2h}
ΔE_{int}	−203.7	−161.3	−224.9
ΔE_{Pauli}	219.1	226.1	349.8
ΔE_{elstat}[a]	−289.1 (68.4%)	−274.0 (70.7%)	−389.9 (67.9%)
ΔE_{orb}[a]	−133.7 (31.6%)	−113.4 (29.3%)	−184.7 (32.1%)
ΔE_{a1g}[b]	−71.8 (53.7%)	−67.0 (59.1%)	−123.2 (66.7%)
ΔE_{b1g}[b]	−8.6 (6.4%)	−6.6 (5.8%)	−9.5 (5.1%)
ΔE_{b2g}[b]	−0.9 (0.7%)	−1.4 (1.3%)	−1.8 (1.0%)
ΔE_{b3g}[b]	−16.9 (12.6%)	−11.0 (9.7 1%)	−15.9 (8.6%)
ΔE_{a1u}[b]	−0.9 (0.7%)	−0.9 (0.7%)	−0.9 (0.5%)
ΔE_{b1u}[b]	−10.8 (8.1%)	−8.3 (7.3%)	−11.0 (6.0%)
ΔE_{b2u}[b]	−20.5 (15.3%)	−15.7 (13.8%)	−19.0 (10.3%)
ΔE_{b3u}[b]	−3.2 (2.4%)	−2.6 (2.3%)	−3.5 (1.9%)
ΔE_{σ}[b]	−92.3 (69.0%)	−82.7 (72.9%)	−142.2 (77.0%)
$\Delta E_{\pi(\parallel)}$[b]	−11.8 (8.8%)	−9.2 (8.1%)	−13.0 (7.0%)
$\Delta E_{\pi(\perp)}$[b]	−27.7 (20.7%)	−19.3 (17.0%)	−27.0 (14.6%)
ΔE_{prep}	8.9	7.0	8.0
$\Delta E(-D_e)$[c]	−194.8	−154.3	−216.9
$-D_o$[c]	−191.0	−150.9	−204.7

Energies are given in kcal/mol.
[a] Values in parentheses give the percentage of the total attractive interactions $\Delta E_{elstat} + \Delta E_{orb}$.
[b] Values in parentheses give the percentage of the total orbital interactions ΔE_{orb}.
[c] The dissociation energy refers to the reaction (**1**)$_2$TM$^+ \rightarrow$ TM$^+ + 2$ **1**.
[d] Values are taken from [15].

The perpendicular and planar structures of the complexes TM(NHC)$_2^+$ were also investigated using the fragmentation into a TM$^+$ cation and a fragment consisting of two carbene ligands. The EDA results are given in Tables 16 and 17. The values for ΔE_{Pauli}, ΔE_{elstat} and ΔE_{orb} are virtually the same for the planar and perpendicular forms. The largest difference is 1.0 kcal/mol for the electrostatic interaction of the gold compounds. The attractive forces are dominated by electrostatic interactions ΔE_{elstat}. The ΔE_{orb} term contributes ~30% to the attractive interactions. Only the planar structure allows for a separation of the orbital interaction ΔE_{orb} in σ, in-plane $\pi_\parallel$ and out-of-plane $\pi_\perp$ interactions. The molecular symmetry of the planar structure is D_{2h}. Orbitals from the a_{1g} and b_{2u} irreducible representations mostly have σ-symmetry, although there are very few δ-orbitals in the a_{1g} representation. More δ-orbitals come from the a_{1u} and b_{2g} irreducible representations. b_{1g} and b_{3u} orbitals belong to in-plane $\pi_\parallel$ symmetry, while b_{1u} and b_{3g} indicate out-of-plane $\pi_\perp$ orbitals. The total σ, $\pi_\parallel$ and $\pi_\perp$ contributions to the orbital interaction are listed in Table 17. The largest part of ΔE_{orb} come from σ orbitals [75], and the in-plane $\pi_\parallel$ contributions account for one third of the total π interaction. The energy resulting from δ orbital interactions is negligible. Thus, the out-of-plane $\pi_\perp$ interactions contribute up to 21% to the orbital interaction energies.

The strength of the out-of-plane $\pi_\perp$ interactions in the planar structures of TM(NHC)$_2^+$ seems surprising considering the very small energy differences (⩽5 kcal/mol)

between the planar and perpendicular forms. The negligible rotational barrier can be explained with the contribution of the in-plane $\pi_{\parallel}$ contributions to the metal–ligand interactions. The EDA results in Tables 16 and 17 show that the sum of $\pi_{\parallel} + \pi_{\perp}$ interactions in the planar form have nearly the same strength as the overall π bonding in the perpendicular form.

The results of the EDA calculations of the group-11 complexes with N-heterocyclic carbenes may be compared with the EDA values for Fischer carbene complexes $(CO)_5Cr–C(X)R$ (Table 2) and $(CO)_5W–C(OH)_2$ (Table 8). The EDA values for the latter complexes suggest that the orbital interactions in typical Fischer complexes contribute between 35% and 40% to the attractive interactions while electrostatic bonding contributes between 60% and 65%. Metal–carbene bonding in group-11 NHC–TMCl complexes has less covalent contributions coming from the ΔE_{orb} term which contributes only between 22% and 26% (Tables 14 and 15). A somewhat surprising result concerns the strength of π bonding in the two classes of carbene complexes. The EDA results suggest that the relative contribution of the $R_2C \leftarrow TML_n$ π-back-donation in the complexes NHC–TMCl is not dramatically smaller than in Fischer carbene complexes which have one or two π-donor groups R. The percentage values for the out-of-plane $\pi_{\perp}$ interactions contribute between 16.1% and 26.6% to the ΔE_{orb} term (Tables 14 and 15). Typical Fischer complexes have values for the $\pi_{\perp}$ interactions between 19% and 35% (Tables 2 and 8). Note, however, that the absolute and relative magnitude of the orbital interactions in NHC–TMCl is smaller than in $(CO)_5TM–C(X)R$.

8. Summary

The theoretical results which are discussed in the work convincingly demonstrate that modern quantum chemical methods may not only give accurate numbers and data for energies, geometries and other observable quantities but they may also give detailed insight into the nature of the bonding situation of transition metal complexes. Charge and energy partitioning devices such as the NBO, CDA, AIM and EDA methods provide a quantitative answer to questions about the bonding situation in terms of simple bonding models which is at the same time in agreement with the physical mechanism of the bond formation. Carbene complexes of Fischer and Schrock types exhibit characteristic differences which become obvious through the calculated data. The contributions of electrostatic and orbital interactions and the strength of the σ and π bonding can be estimated using unambigiously defined quantum chemical expressions. The results of the bonding analyses may help to establish a well defined ordering scheme for the variety of carbene complexes which are formed between carbene ligands and metal fragments having different electronic structures. It is possible to understand the chemical properties of the different carbene complexes through quantum chemical analyses of the electronic structure. The results of the bonding analyses show that heuristic bonding models which were proven to be helpful in the past may not be discarded. Rather, they become qualitatively and quantitatively supported by the well defined quantum chemical partitioning methods.

Acknowledgments

This work was supported by the Deutsche Forschungsgemeinschaft and the Spanish MCyT Project No. BQU2002-0412-C02-02. M.S. is indebted to the DURSI of the Generalitat de Catalunya for financial support through the Distinguished University Research Promotion, 2001. Excellent service by the Hochschulrechenzentrum of the Philipps-Universität Marburg is gratefully acknowledged. Additional computer time was provided by the HLRS Stuttgart, HHLRZ Darmstadt, and the Centre de Supercomputació de Catalunya (CESCA).

References

[1] E.O. Fischer, A. Maasböl, Angew. Chem. 76 (1964) 645; Angew. Chem., Int. Ed. Engl. 3 (1964) 580.
[2] (a) K.H. Dötz, H. Fischer, P. Hofmann, F.R. Kreissl, U. Schubert, K. Weiss, Transition Metal Carbene Complexes, VCH, Weinheim, 1983;
(b) K.H. Dötz, Angew. Chem. 96 (1984) 573; Angew. Chem., Int. Ed. Engl. 23 (1984) 587;
(c) L.S. Hegedus, in: E.W. Abel, F.G.A. Stone, G. Wilkinson (Eds.), Comprehensive Organometallic Chemistry II, vol. 12, Pergamon Press, Oxford, 1995, p. 549;
(d) F.G.A. Wulff, in: B.M. Trost, I. Fleming (Eds.), Comprehensive Organic Synthesis, vol. 5, Pergamon Press, Oxford, 1991, p. 1065;
(e) W.D. Wulff, in: E.W. Abel, F.G.A. Stone, G. Wilkinson (Eds.), Comprehensive Organometallic Chemistry II, Pergamon Press, Oxford, 1995, p. 469;
(f) D.F. Harvey, D.M. Sigano, Chem. Rev. 96 (1996) 271;
(g) A. de Meijere, Pure Appl. Chem. 68 (1996) 61;
(h) J. Barluenga, Pure Appl. Chem. 68 (1996) 543;
(i) R. Aumann, H. Nienaber, Adv. Organomet. Chem. 41 (1997) 163;
(j) K.H. Dötz, P. Tomuschat, Chem. Soc. Rev. 28 (1999) 187;
(k) M.A. Sierra, Chem. Rev. 100 (2000) 3591;
(l) M.W. Davies, C.N. Johnson, J.P.A. Harrity, J. Org. Chem. 66 (2001) 3525;
(m) J. Barluenga, A.L. Suárez-Sobrino, M. Tomás, S. García-Granda, R. Santiago-García, J. Am. Chem. Soc. 123 (2001) 10494;
(n) J. Barluenga, Pure Appl. Chem. 71 (1999) 1385.
[3] R.R. Schrock, J. Am. Chem. Soc. 96 (1974) 6796.
[4] (a) W.A. Nugent, J.M. Mayer, Metal–Ligand Multiple Bonds, Wiley, New York, 1988;
(b) R.R. Schrock, Chem. Rev. 102 (2002) 145.
[5] (a) M.J.S. Dewar, Bull. Soc. Chim. Fr. 18 (1951) C79;
(b) J. Chatt, L.A. Duncanson, J. Chem. Soc. (1953) 2929.
[6] T.E. Taylor, M.B. Hall, J. Am. Chem. Soc. 106 (1984) 1576.
[7] (a) K. Öfele, J. Organomet. Chem. 12 (1968) P42;
(b) K. Öfele, E. Roos, M. Herberhold, Z. Naturforsch. B 31 (1976) 1070.
[8] (a) H.-W. Wanzlick, H.-J. Schönherr, Angew. Chem. 80 (1968) 154;
(b) Angew. Chem., Int. Ed. Engl. 7 (1968) 141.
[9] (a) W.A. Herrmann, C. Köcher, Angew. Chem. 109 (1997) 2257;
(b) Angew. Chem., Int. Ed. Engl. 36 (1997) 2162.
[10] G. Frenking, N. Fröhlich, Chem. Rev. 100 (2000) 717.

[11] P. Hofmann, in: K.H. Dötz, H. Fischer, P. Hofmann, F.R. Kreissl, U. Schubert, K. Weiss (Eds.), Transition Metal Carbene Complexes, Verlag Chemie, Weinheim, 1983, p. 118.
[12] M. Cases, G. Frenking, M. Duran, M. Solà, Organometallics 21 (2002) 4182.
[13] M. Lein, A. Szabó, A. Kovács, G. Frenking, Faraday Discuss. 124 (2003) 365.
[14] S.F. Vyboishchikov, G. Frenking, Chem. Eur. J. 4 (1998) 1428.
[15] D. Nemcsok, K. Wichmann, G. Frenking, Organometallics 23 (2004) 3640.
[16] C. Boehme, G. Frenking, Organometallics 17 (1998) 5801.
[17] S. Dapprich, G. Frenking, J. Phys. Chem. 99 (1995) 9352.
[18] (a) G. te Velde, F.M. Bickelhaupt, E.J. Baerends, C. Fonseca Guerra, S.J.A. Van Gisbergen, J.G. Snijders, T. Ziegler, J. Comput. Chem. 22 (2001) 931;
(b) F.M. Bickelhaupt, E.J. Baerends, Rev. Comput. Chem. 15 (2000) 1.
[19] T. Ziegler, A. Rauk, Theoret. Chim. Acta 46 (1977) 1.
[20] (a) K. Morokuma, J. Chem. Phys. 55 (1971) 1236;
(b) K. Kitaura, K. Morokuma, Int. J. Quantum Chem. 10 (1976) 325.
[21] (a) R.F.W. Bader, Atoms in Molecules: A Quantum Theory, Oxford University Press, Oxford, 1990;
(b) R.F.W. Bader, in: P.v.R. Schleyer, N.L. Allinger, P.A. Kollmann, T. Clark, H.F.S. Schaefer, J. Gasteiger, P.R. Schreiner (Eds.), Encyclopedia of Computational Chemistry, vol. 1, Wiley–VCH, Chichester, 1998, p. 64.
[22] A.E. Reed, L.A. Curtiss, F. Weinhold, Chem. Rev. 88 (1988) 899.
[23] (a) T.R. Cundari, M.S. Gordon, J. Am. Chem. Soc. 113 (1991) 5231;
(b) T.R. Cundari, M.S. Gordon, J. Am. Chem. Soc. 114 (1992) 539;
(c) T.R. Cundari, M.S. Gordon, J. Phys. Chem. 96 (1992) 631;
(d) T.R. Cundari, M.S. Gordon, Organometallics 11 (1992) 3122.
[24] (a) H. Jacobsen, G. Schreckenbach, T. Ziegler, J. Phys. Chem. 98 (1994) 11406;
(b) H. Jacobsen, T. Ziegler, Organometallics 14 (1995) 224;
(c) H. Jacobsen, T. Ziegler, Inorg. Chem. 35 (1996) 775.
[25] (a) H. Nakatsuji, M. Hada, K. Kondo, Chem. Phys. Lett. 196 (1992) 404;
(b) A. Márquez, J.F. Sanz, J. Am. Chem. Soc. 114 (1992) 2903;
(c) A. Márquez, J.F. Sanz, J. Am. Chem. Soc. 114 (1992) 10019;
(d) W.W. Schoeller, D. Eisner, S. Grigoleit, A.B. Rozhenko, A. Alijah, J. Am. Chem. Soc. 122 (2000) 10115;
(e) X. Hu, I. Castro-Rodriguez, K. Olsen, K. Meyer, Organometallics 23 (2004) 755;
(f) M.-T. Lee, C.-H. Hu, Organometallics 23 (2004) 976;
(g) I. Fernández, F.P. Cossío, A. Arrieta, B. Lecea, M.J. Mancheo, M.A. Sierra, Organometallics 23 (2004) 1065.
[26] (a) C. Møller, M.S. Plesset, Phys. Rev. 46 (1934) 618;
(b) J.S. Binkley, J.A. Pople, Int. J. Quantum Chem. 9S (1975) 229.
[27] (a) J. Cizek, J. Chem. Phys. 45 (1966) 4256;
(b) J. Cizek, Adv. Chem. Phys. 14 (1966) 35;
(c) J.A. Pople, R. Krishnan, H.B. Schlegel, J.S. Binkley, Int. J. Quantum Chem. 14 (1978) 545;
(d) R.J. Bartlett, G.D. Purvis, Int. J. Quantum Chem. 14 (1978) 561;
(e) G.D. Purvis, R.J. Bartlett, J. Chem. Phys. 76 (1982) 1910;
(f) J. Noga, R.J. Bartlett, J. Chem. Phys. 86 (1987) 7041;
(g) K. Raghavachari, G.W. Trucks, J.A. Pople, M. Head-Gordon, Chem. Phys. Lett. 157 (1989) 479.
[28] (a) A.D. Becke, Phys. Rev. A 38 (1988) 3098;
(b) J.P. Perdew, Phys. Rev. B 33 (1986) 8822;
J.P. Perdew, Phys. Rev. B 34 (1986) 7406.
[29] (a) A.D. Becke, J. Chem. Phys. 98 (1993) 5648;
(b) C. Lee, W. Yang, R.G. Parr, Phys. Rev. B 37 (1988) 785;
(c) P.J. Stevens, F.J. Devlin, C.F. Chabalowski, M.J. Frisch, J. Phys. Chem. 98 (1994) 11623.
[30] (a) C. Chang, M. Pelissier, Ph. Durand, Phys. Scr. 34 (1986) 394;
(b) J.-L. Heully, I. Lindgren, E. Lindroth, S. Lundquist, A.-M. Martensson-Pendrill, J. Phys. B 19 (1986) 2799;
(c) E. van Lenthe, E.J. Baerends, J.G. Snijders, J. Chem. Phys. 99 (1993) 4597;
(d) E. van Lenthe, E.J. Baerends, J.G. Snijders, J. Chem. Phys. 105 (1996) 6505;
(e) E. van Lenthe, R. van Leeuwen, E.J. Baerends, J.G. Snijders, Int. J. Quantum Chem. 57 (1996) 281.
[31] G. Frenking, I. Antes, M. Boehme, S. Dapprich, A.W. Ehlers, V. Jonas, A. Neuhaus, M. Otto, R. Stegmann, A. Veldkamp, S.F. Vyboishchikov, in: K.B. Lipkowitz, D.B. Boyd (Eds.), Reviews in Computational Chemistry, vol. 8, VCH, New York, 1996, pp. 63–144.
[32] For a short description of the NBO procedure see also [10], p. 728.
[33] F. Maseras, K. Morokuma, Chem. Phys. Lett. 195 (1992) 500.
[34] (a) U. Pidun, G. Frenking, J. Organomet. Chem. 525 (1996) 269;
(b) U. Pidun, G. Frenking, J. Chem. Soc., Dalton Trans. (1997) 1653.
[35] S.A. Decker, M. Klobukowski, J. Am. Chem. Soc. 1201 (1998) 9342.
[36] T.S. Slee, J. Am. Chem. Soc. 108 (1986) 7541.
[37] J. Cioslowski, S.T. Mixon, J. Am. Chem. Soc. 113 (1991) 4142.
[38] (a) X. Fradera, M.A. Austen, R.F.W. Bader, J. Phys. Chem. A 103 (1999) 304;
(b) X. Fradera, J. Poater, S. Simon, M. Duran, M. Solà, Theoret. Chem. Acc. 108 (2002) 214.
[39] (a) R. Bochicchio, R. Ponec, A. Torre, L. Lain, Theoret. Chem. Acc. 105 (2001) 292;
(b) R. Bochicchio, L. Lain, A. Torre, R. Ponec, J. Math. Chem. 28 (2000) 83.
[40] (a) R. Bochicchio, R. Ponec, A. Torre, L. Lain, Theoret. Chem. Acc. 105 (2001) 292;
(b) R. Ponec, I. Mayer, J. Phys. Chem. A 101 (1997) 1738.
[41] K. Ruedenberg, Rev. Mod. Phys. 34 (1962) 326.
[42] W. Heitler, F. London, Z. Physik 44 (1927) 455.
[43] The preparation energy may also include electronic excitation energy if the electronic ground state of the fragment is different from the electronic reference state in the molecule.
[44] F.M. Bickelhaupt, N.M.M. Nibbering, E.M. van Wezenbeek, E.J. Baerends, J. Phys. Chem. 96 (1992) 4864.
[45] D. Cappel, S. Tüllmann, A. Krapp, G. Frenking, Angew. Chem. 117 (2005) 3683;
Angew. Chem., Int. Ed. Engl. 44 (2005) 3617.
[46] (a) R. Ahlrichs, M. Bär, M. Häser, H. Horn, C. Kölmel, Chem. Phys. Lett. 162 (1989) 165;
(b) O. Treutler, R. Ahlrichs, J. Chem. Phys. 102 (1995) 346.
[47] ACES-II is a package of ab initio programs written by J.F. Stanton, J. Gauss, J.D. Watts, W.J. Lauderdale, R.J. Bartlett. For details see: www.aces2.de.
[48] (a) M.J. Frisch, G.W. Trucks, H.B. Schlegel, G.E. Scuseria, M.A. Robb, J.R. Cheeseman, V.G. Zakrzewski, J.A. Montgomery, R.E. Stratmann, J.C. Burant, S. Dapprich, J.M. Milliam, A.D. Daniels, K.N. Kudin, M.C. Strain, O. Farkas, J. Tomasi, V. Barone, M. Cossi, R. Cammi, B. Mennucci, C. Pomelli, C. Adamo, S. Clifford, J. Ochterski, G.A. Petersson, P.Y. Ayala, Q. Cui, K. Morokuma, D.K. Malick, A.D. Rabuck, K. Raghavachari, J.B. Foresman, J. Cioslowski, J.V. Ortiz, B.B. Stefanov, G. Liu, A. Liashenko, P. Piskorz, I. Komaromi, R. Gomberts, R.L. Martin, D.J. Fox, T.A. Keith, M.A. Al-Laham, C.Y. Peng, A. Nanayakkara, C. Gonzalez, M. Challacombe, P.M.W. Gill, B.G. Johnson, W. Chen, M.W. Wong, J.L. Andres, M. Head-Gordon, E.S. Replogle, J.A. Pople, GAUSSIAN-98, Gaussian, Inc., Pittsburgh, PA, 1998;
(b) M.J. Frisch, G.W. Trucks, H.B. Schlegel, G.E. Scuseria, M.A. Robb, J.R. Cheeseman, J.A. Montgomery Jr., T. Vreven, K.N. Kudin, J.C. Burant, J.M. Milliam, S.S. Iyengar, J. Tomasi, V. Barone, B. Mennucci, M. Cossi, G. Scalmani, N. Rega, G.A. Petersson, H. Nakatsuji, M. Hada, M. Ehara, K. Toyota, R. Fukuda, J. Hasegawa, M. Ishida, T. Nakajima, Y. Honda, O. Kitao, H. Nakai, M. Klene, X. Li, J.E. Knox, H.P. Hratchian, J.B. Cross, C. Adamo, J. Jaramillo, R. Gomperts, R.E. Stratmann, O. Yazyev, A.J. Austin, R. Cammi, C. Pomelli, J.W. Ochterski, P.Y. Ayala, K. Morokuma, G. Voth, P. Salvador, J.J. Dannenberg, V.G. Zakrzewski, S. Dapprich, A.D. Daniels, M.C. Strain, O. Farkas, D.K. Malick, A.D. Rabuck, K.

Raghavachari, J.B. Foresman, J.V. Ortiz, Q. Cui, A.G. Baboul, S. Clifford, J. Cioslowski, B.B. Stefanov, G. Liu, A. Liashenko, P. Piskorz, I. Komaromi, R.L. Martin, D.J. Fox, T. Keith, M.A. Al-Laham, C.Y. Peng, A. Nanayakkara, M. Challacombe, P.M.W. Gill, B. Johnson, W. Chen, C. Wong, M.W. Gonzalez, J.A. Pople, GAUSSIAN-03, Gaussian, Inc., Pittsburgh, PA, 2003.

[49] CDA-2.1 is a program written by S. Dapprich, and G. Frenking, It is available via anonymous ftp server: ftp.chemie.uni-marburg.de(/pub/cda).

[50] AIMPAC Program Package, R.F.W. Bader research group, McMaster University, Hamilton, Canada.

[51] R.D. Topsom, Acc. Chem. Res. 18 (1983) 292.

[52] C. Hansch, A. Leo, R.W. Taft, Chem. Rev. 91 (1991) 165.

[53] A.W. Ehlers, S. Dapprich, S.F. Vyboishchikov, G. Frenking, Organometallics 15 (1996) 105.

[54] G. Frenking, K. Wichmann, N. Fröhlich, C. Loschen, M. Lein, J. Frunzke, V.M. Rayón, Coord. Chem. Rev. 238–239 (2003) 55.

[55] M.A. Spackman, E.N. Maslen, J. Phys. Chem. 90 (1986) 2020.

[56] C. Esterhuysen, G. Frenking, Theoret. Chem. Acc. 111 (2004) 381.

[57] A. Kovács, C. Esterhuysen, G. Frenking, Chem. Eur. J. 11 (2005) 1813.

[58] W. Kutzelnigg, in: Z.B. Maksic (Ed.), The Concept of the Chemical Bond: Part 2, Springer, Berlin, 1990, p. 5f.

[59] A case where the trend of the overall bond strength becomes determined by the electrostatic term has recently been reported for phosphane complexes $(CO)_5TM–PR_3$: G. Frenking, K. Wichmann, N. Fröhlich, J. Grobe, W. Golla, D. Le Van, B. Krebs, M. Läge, Organometallics 21 (2002) 2921.

[60] Ch. Elschenbroich, A. Salzer, in: Organometallics: A Concise Introduction, second ed., VCH, Weinheim, 1992, p. 214.

[61] R.G. Parr, L.v. Szentpály, S. Liu, J. Am. Chem. Soc. 121 (1999) 1922.

[62] (a) R.G. Parr, W. Yang, Density-Functional Theory of Atoms and Molecules, Oxford University Press, New York, 1989;
(b) R.G. Pearson, Chemical Hardness, Wiley–VCH, Oxford, 1997.

[63] J. Poater, M. Cases, X. Fradera, M. Duran, M. Solà, Chem. Phys. 294 (2003) 129.

[64] (a) C.-C. Wang, Y. Wang, H.-J. Liu, K.-J. Lin, L.-K. Chou, K.-S. Chan, J. Phys. Chem. A 101 (1997) 8887;
(b) T.F. Block, R.F. Fenske, J. Am. Chem. Soc. 99 (1977) 4321.

[65] T. Kar, J.G. Ángyán, A.B. Sannigrahi, J. Phys. Chem. A 104 (2000) 9953.

[66] D. Cremer, E. Kraka, Angew. Chem. 96 (1984) 612;
Angew. Chem., Int. Ed. Engl. 23 (1984) 627.

[67] The bond ellipticity at the bond critical point ε_c is defined by the ratio of the curvatures (eigenvalues of the Hessian of $\rho(\mathbf{r}_c)$) along the two axes perpendicular to the bond less one: $\varepsilon = \max(\lambda_1, \lambda_2)/\min(-\lambda_1, \lambda_2) - 1$. For details see [21].

[68] U. Schubert, Coord. Chem. Rev. 55 (1984) 261.

[69] There are two mirror planes in C_{2v} symmetry. The genuine π-back-donation shown in Fig. 1(a) refers to orbitals having b_1 symmetry in. This is the $\pi_\perp$-interaction. The b_2 orbital contributions come from in-plane ($\pi_\parallel$) interactions.

[70] P. Pykkö, Chem. Rev. 88 (1988) 563.

[71] P. Schwerdtfeger, P.D.W. Boyd, A.K. Burrell, W.T. Robinson, M.J. Taylor, Inorg. Chem. 29 (1990) 3593.

[72] C. Boehme, Ph.D. Thesis, Marburg, 1998.

[73] A.J. Arduengo, H.V.R. Dias, J.C. Calabrese, F. Davidson, Organometallics 12 (1993) 3405.

[74] P.v.R. Schleyer, C. Maerker, A. Dransfeld, H. Jiao, N.E. Hommes, J. Am. Chem. Soc. 118 (1996) 6317.

[75] The authors took the sum of a_{1g} and b_{2u} irreducible representations for the energy coming from σ-orbitals.